



6th USWNet Conference

Nov. 13th-14th 2008
ETH Zurich, Switzerland

Fluid and particle manipulation with physical force fields for
medical micro-system applications

Book of abstracts

Preface

The USWNet conferences are select meetings for a diversity of scientists and technologist with interests touching on particle and fluid movement in standing wave vibrations. You are invited to send abstracts and register for this meeting now. Registration and abstract submission forms can be downloaded from the USWNet website

<http://www.ucl.ac.uk/medicine/hepatology-rf/research/usw-net/>

The meeting will include invited talks from the parallel fields of dielectrophoresis (Dr. M. S. Jäger) and optical traps (Dr. M. Goksör) and therefore cover a wide number of forces which act on particles and fluids. Taken together the control of force field phenomena provide many technological possibilities. The conference is aimed at fostering a deeper understanding of the phenomena and increasing their impact into commercial avenues and particularly forces acting on cells for medical applications.

Who should come to the conference? Anyone with interests or application needs in the following areas:

- Control of biological cells and particles in water, air or other fluids
- Clumping; filtration, separation, cell washing, perfusion, agglutination and cell-cell communication
- Cell positioning; on biosensor surfaces, in tissue engineering structures. Rapid detection methods
- Streaming of fluids and or particles; Mixing, breaking through boundary layers and laminar flow regimes, surface cleaning, reaction rate enhancement
- Cell sonoporation and disruption; drug delivery, cell content extraction.

Note: in the following week (17th-19th Nov. 2008) the Nanotech Montreux conference is taking place in Montreux, Switzerland (<http://www.nanotech-montreux.com>). If you have an interest microfluidic technology you may wish to take advantage of this juxtaposition and attend both meetings. Please note that Nanotech Montreux is not taking place the same week as USWNet 2008, as previously announced in the 1st call for papers.

The conference organizers:

Stefano Oberti, ETH Zurich
Jürg Dual, ETH Zurich
Jeremy Hawkes, The University of Manchester
Martin Wiklund, KTH Stockholm
Rosemary Townsend, University of Southampton
Martyn Hill, University of Southampton

Co-organizer:



Acknowledgements

The USWNet 2008 organization committee would like to express its gratitude to F. Hoffmann-La Roche Ltd for the sponsorship and the Micro and Nano Science Platform of ETH Zurich for the co-organization of the event.



Day 1 (13th Nov. 2008)

Registration

12:00 – 14:00, CLA J5

Welcome speech (Prof. Dr. J. Dual, S. Oberti)

14:00 – 14:10, CLA J1

Invited talk (Chair: Prof. Dr. J. Dual)

14:10 – 15:00

Optical Manipulation: Principles and Applications in Life Sciences

M. Goksör, Göteborg University

Session 1 – Manipulation strategies, advanced fields (Chair: Prof. Dr. J. Dual)

15:00 – 15:20

Alleviating Problems With Clogging And Trapping In Microchannel Ultrasonic

Standing Wave Separation: A Multiple Node Approach For Complex Bio-

Suspensions

Carl Grenvall, Lund University

15:20 – 15:40

Multidimensional Ultrasonic Manipulation Stabilized by Frequency Modulation

Otto Manneberg, KTH Stockholm

Session 2 – Bioapplications 1 (Chair: Prof. Dr. T. Laurell)

15:40 – 16:00

Affinity Extraction of Antibodies using Acoustophoresis

Per Augustsson, Lund University

16:00 – 16:20

Fractionation of microparticles with acousto-optically generated potential

energy landscapes

Michael P. MacDonald, University of Dundee

Break (and posters)

16:20 – 16:40, CLA J5

Session 3 – Related phenomena 1 (Chair: Prof. Dr. M. Hill)

16:40 – 17:00

Changes of Bubble Dynamics revealed through Optical Micromanipulation of

Ultrasound Contrast Agent Microbubbles

Michel Versluis, University of Twente

17:00 – 17:20

Electrothermal and Electroosmotic Fluid Flow Induced in a Dielectrophoretic

Deposition Device

Brian Burg, ETH Zurich

Introduction to USWNet and its website (Dr. R. Boltryk)

17:20 – 17:30

Break

17:30 – 17:40, CLA J5

Session 4 – Manipulation strategies, advanced fields 2 (Chair: Prof. Dr. M. Hill)

17:40 – 18:00

Experimental study of particle motion within a microchannel narrower than half

a wavelength

Itziar Gonzales, Instituto de Acústica Madrid

18:00 – 18:20

Towards a Binary Particle Fractionator

Nick Harris, University of Southampton

18:20 – 18:40

Two dimensional acoustic standing fields in open and closed systems

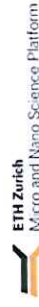
Stefano Oberti, ETH Zurich

Lab Tour at Center of Mechanics (Prof. J. Dual, S. Oberti)

18:40 – 19:20, CLA H-floor (meeting point CLA H22)

Dinner

19:30 - ..., meeting point in front of CLA building (Clausiusstrasse)



Day 2 (14th Nov. 2008)

Invited talk (Chair: Dr. M. Wiklund)

08:00 – 08:50, CLA J1
Single-particle control by electric fields: from living cells to viruses and nanowires
 M. S. Jäger, Fraunhofer Institute for Biomedical Engineering (IBMT)

Session 5 – Related Phenomena 2 (Chair: Dr. M. Wiklund)

08:50 – 09:10
Infrared absorbance spectra of water influenced by an ultrasonic standing wave
 Stefan Radel, Vienna University of Technology

09:10 – 09:30

Effective mixing of laminar flows at a density interface by an integrated ultrasonic transducer
 Linda Johansson, Uppsala University

09:30 – 09:50

Acoustic streaming at ultrasound resonances in microfluidic chambers: theory and simulation
 Henrik Bruus, Technical University of Denmark

09:50 – 10:10

Acoustic streaming: The main driving mechanism for particle clump formation in MHz ultrasonic standing waves
 Jeremy Hawkes, The University of Manchester

Break (and posters)

10:10 – 10:30, CLA J5

Session 6 – Theoretical analysis, modelling (Chair: Dr. R. Boltryk)

10:30 – 10:50

1-Dimensional Transducer model for performance studies of ultrasonic standing waves in arbitrary stacks of PZT, liquid and solid layers
 Frederic Cegla, Imperial College London

10:50 – 11:10

Numerical simulations for the time-averaged acoustic forces acting on rigid cylinders in ideal and viscous fluids
 Jingtao Wang, ETH Zurich

Break

11:10 – 11:20, CLA J5

Session 7 – Bioapplications 2 (Chair: Prof. Dr. T. Laurell)

11:20 – 11:40
Multi-modal particle manipulation with integrated optical waveguide detection
 P. Glynne-Jones, University of Southampton

11:40 – 12:00

A bioassay for monitoring ATP release in RBC agglomerates
 Björn Hammarström, Lund University

12:00 – 12:20

Chip-integrated Confocal Ultrasonic Resonator for Selective Bioparticle Manipulation
 Jessica Svennebring, KTH Stockholm

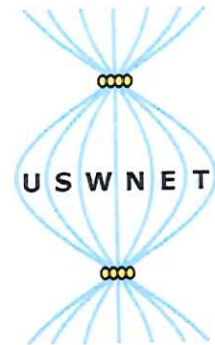
Closing remarks (Dr. J. Hawkes)

12:20 – 12:30

Optical Manipulation; Principles and Applications in Life Science

Mattias Goksör¹

¹Department of Physics
Göteborg University
SE-41296 Göteborg
Sweden
mattias.goksor@physics.gu.se



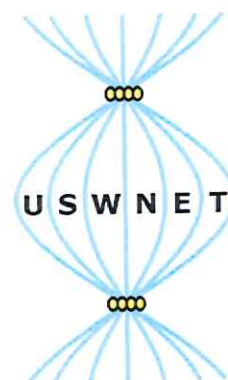
Optical tweezers are a laser based non-invasive manipulation technique for trapping microscopic objects and cells without any physical contact. The optical tweezers are constructed by focusing a laser beam with a powerful lens (such as a high NA microscope objective) into a diffraction-limited spot. The result is a three dimensional trapping potential in which particles can be held. This technique has during the last decade be applied in different disciplines within the life sciences, and has proven especially useful for studies of single cells with high spatial and temporal control. As long as the trapped cell is transparent to the wavelength of the trapping laser light the cell can be trapped for an extended period of time without any optically induced damages. A laser scalpel (or laser microbeam) is in a similar manner created by focusing a pulsed UV (or IR fs) laser light. The absorption of the light creates a highly localized microplasm that can induce pores in membranes or cut chromosomes inside living cells.

In this presentation I will give a brief overview of the principles behind different optical manipulation techniques. I will also demonstrate how we have applied optical manipulation for specific research questions in life science.

Alleviating Problems With Clogging And Trapping In Microchannel Ultrasonic Standing Wave Separation: A Multiple Node Approach For Complex Bio-Suspensions

Carl Grenvall¹, Per Augustsson¹,

Hideaki Matsuoka² and Thomas Laurell¹



¹Div. Nanobiotechnology
Dept. Electrical Measurements
Lund University
Lund
Sweden
carl.grenvall@elmat.lth.se

²Matsuoka Laboratory
Dept. Life Science and Biotechnology
Tokyo University of Agriculture and Technology
Tokyo
Japan

A microchip for multiple node separation of particles was developed. The combination of multiple node acoustic standing waves and sheath flows demonstrates a mode of operation that avoids the problem of lipid particle aggregation along the sidewalls, with subsequent loss in separation performance, in previously reported single node ($\lambda/2$) standing wave systems. The design also solves the problem of separation performance loss due to Rayleigh streaming (RS) in systems with large differences in acoustic separation force, e.g. systems with large differences in particle size¹. The proposed methodology is developed for the separation of bacterial species from foodstuff samples to enable high-speed (≤ 10 min/sample) quality control in industrial food production.

Acoustic particle manipulation is a gentle and robust way of handling particles in microfluidic networks. The acoustic radiation force induced on the particles allows for sorting, trapping and valveless switching of particles². Successful in field cell culturing during and viability studies post exposure to the acoustic field has been performed^{3, 4}. The method does however have some intrinsic difficulties when it comes to handling of small particles and high particle concentrations.

Trapping at surfaces with low shear rate and RS caused by the need of higher acoustic power will set the lower size limit for separation of particles in $\lambda/2$ systems. Both problems are caused by decreasing acoustic radiation forces coupled to decreasing particle size. An adequate example would be raw milk handling where the ability to remove the emulsified lipid fraction is important for rapid bacterial content analysis. When trying to separate the bacteria in a standard $\lambda/2$ separator the input acoustic power required to move bacteria would either cause the lipids to be trapped on the channel side walls or RS to disperse the bacteria laterally across the whole channel width, both cases leading to erroneous separation.

This paper proposes the use of multiple standing wave node systems to solve these problems. Initially a $\lambda/2$ reference channel matched to 2 MHz was investigated. Subsequently channels matching $2\lambda/2$ and $3\lambda/2$ widths respectively at 2 MHz were employed to alleviate problems of lipid emulsion trapping. The channels were supplied with three in- and outlets. A test sample containing 3% milk lipid suspension and 0.1% small particles (red 3 μm polystyrene (rPS)) was used for the investigations.

¹ J. Hawkes, R. Barber, D. Emerson and W. Coakley, Lab Chip (4) 446-452, 2004

² T. Laurell, F. Petersson and A. Nilsson, Chem Soc Rev (36) 492-506, 2007

³ J. Hultström, O. Manneberg, K Dopf et al, Ultrasound Med Biol 33 (1) 145-151, 2007

⁴ M. Evander, L. Johansson, T. Lillichorn, J. Piskur, M. Lindvall, S. Johansson, M. Almqvist, T. Laurell and J. Nilsson, Anal Chem (79) 2984-2991, 2007

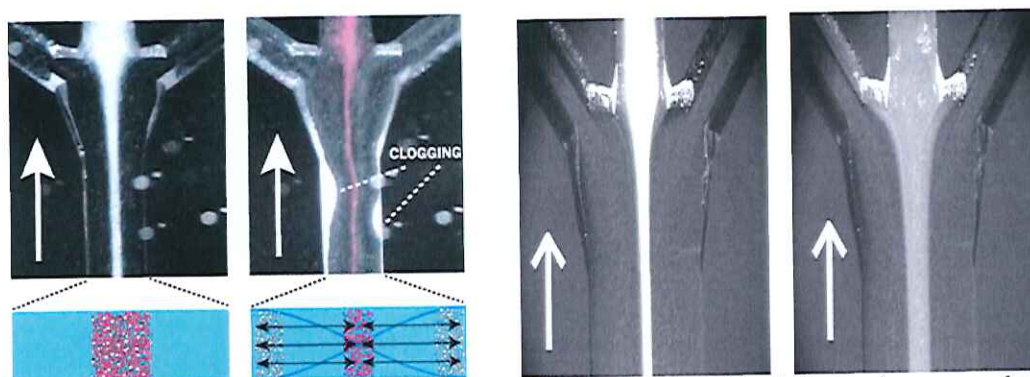


Fig. 1, Problems involved with ultrasonic standing wave particle manipulation. Left hand pictures from a normal microscope illustrate lipid clogging as ultrasound (US) is activated in a $\lambda/2$ channel (far left US off, middle left US on) used to separate red polystyrene particles from lipids. Right hand pictures from a fluorescent microscope demonstrate the problem with RS in a $2\lambda/2$ channel (middle right US off, far right US on) which causes $0.87\ \mu\text{m}$ fluorescein isothiocyanate (FITC)-marked polystyrene particles to spread out across the channel instead of focusing in two lines, both halfway to either side (FITC used to improve visualization).

The $\lambda/2$ channel rapidly clogged when running the test sample, Fig 1 left. The $2\lambda/2$ channel prevented clogging as lipids were focused in the channel centre with high flow rate. The additional nodes acted as acoustic barriers through which no particles could reach the sidewalls, Fig 2 left. However, when running $0.87\ \mu\text{m}$ FITC-marked polystyrene particles in the $2\lambda/2$ channel, RS and low acoustic radiation forces prevented separation, Fig 1 right. The final solution emerged in a $3\lambda/2$ channel, which managed to separate lipids from rPS without having to move the rPS, making the system independent of small particle size, Fig 2 right. This is our first proof of concept of a microfluidic sample preparation chip for food stuff bacterial content analysis.

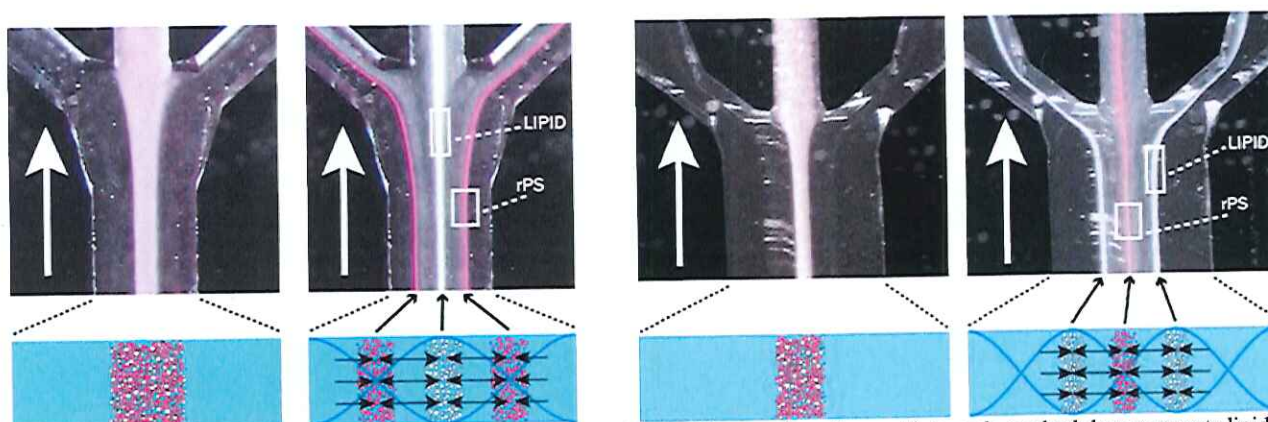


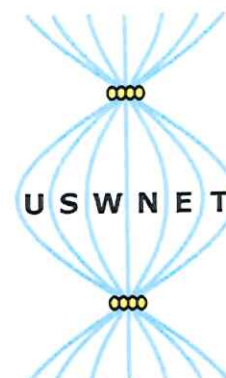
Fig. 2, Solutions to the problems described earlier. Left hand pictures illustrate how the multiple node methodology prevents lipid clogging along the sidewalls in a $2\lambda/2$ wide microchannel. By introducing additional ultrasonic nodes which act as acoustic barriers the particles are prevented from spreading out across the channel, thus creating sheath flows along the sides (far left US off, middle left US on). Right hand pictures illustrate the final solution which use sheath flows while avoiding the problem with RS by making the channel independent of ultrasonic forces acting on sub micrometer particles (middle right US off, far right US on).

The authors would like to thank VINNOVA, the Royal Physiographic Society and the Crafoord Foundation for funding and support.

Multidimensional Ultrasonic Manipulation Stabilized by Frequency Modulation

Otto Manneberg, Johan Strååt and Martin Wiklund

Royal Inst. of Technology (KTH)
Dept. of Applied Physics.
KTH/AlbaNova
SE-10691 Stockholm
Sweden
otto.manneberg@biox.kth.se



Ultrasonic standing wave (USW) manipulation of cells or bio-functionalized beads in microfluidic chips has been proven to be a simple and gentle method.¹ However, the direct contact of the transducer to the system can result in changes of resonance frequency over time due to heating from mechanical losses in, e.g., the piezoelectric element.² Furthermore, single-frequency USW excitation in chips typically results in a non-uniform force field along the microchannel.^{3,4} The former effect can be mitigated by the fact that, e.g., a microfluidic chip for USW manipulation is resonant over a range of frequencies, with different excitation frequencies giving different nodal patterns (as shown in Refs. 3-4), so that a change in temperature still allows a significant force field, albeit a different one. Still, long-term stability and generation of controlled force fields remain a problem.

We have previously shown that it is possible to spatially confine a 3D ultrasonic force field to a predetermined section of a microchannel⁵ or a microcage⁶, enabling different manipulation functions to be carried out in different parts of the same chip. In the present work, we use high-rate (~ 1 kHz) frequency-modulated excitation signals to stabilize the manipulation performance both spatially and temporally, and low-rate (~ 0.1 Hz) frequency modulation to transport particle aggregates or single particles in a microchannel without medium flow.

We employ a fully transparent glass-silicon-glass chip with a coverslip-thick bottom plate, enabling all kinds of high-resolution optical microscopy. The system is excited using external, exchangeable wedge transducers³ giving complete freedom in choice of excitation frequency.

Figure 1 shows the effect of frequency modulation (a sawtooth wave modulated in the vicinity of 2 MHz with a rate of 1 kHz) of the excitation signal in a 25 mm long straight channel. The images were taken by seeding the channel homogeneously with a high concentration of 5- μ m polyamide particles, letting the ultrasound act for 20 seconds to produce a stationary pattern and then imaging the entire channel. Figures 1a-b show the effect at room temperature, and Figs. 1c-d at 37° C. In both cases, we note that the pattern is more uniform when stabilized (Figs. 1b and 1d).

The effect can also be used to employ one transducer for two manipulation functions requiring slightly different frequencies, such as focusing and levitating beads simultaneously in a square channel. This is otherwise difficult due to the complex structure of the resonances in the chip. Figure 2 shows how this is utilised in pre-aligning particles for trapping in an ultrasonic microcage.

Finally, in Fig. 3 we demonstrate how a slow frequency modulation (a sawtooth wave with a rate of 0.1-0.2 Hz) can be employed to transport both aggregates of 5- μ m polyamide particles (not shown here) and single 10- μ m microbeads into a microcage, where they are trapped and held in three dimensions. The technology is based on the fact that a small frequency shift gives a small shift in the nodal locations. The lack of medium flow is demonstrated by introducing tracer particles too small to be trapped by the ultrasound (not shown here).

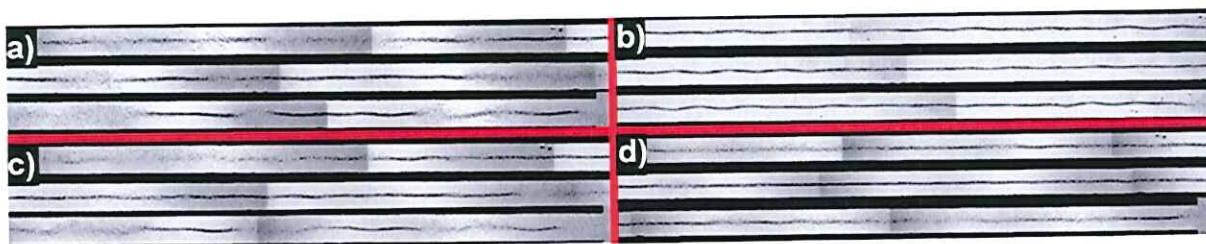


Fig. 1: The effect of frequency modulation on particle patterns in a straight 25 mm long channel. Images wrap so that the right end of an upper one connects to the left of a lower. Fig. 1a shows the pattern at 1.97 MHz and 6 volts peak-to-peak (V_{pp}) at room temperature (23° C). Fig. 1b shows the pattern stabilized by frequency modulation (sweep between 1.87-1.97 MHz at 1 kHz), with the voltage at 10 V_{pp} . Figure 1c shows the pattern at 1.97 MHz and 6 V_{pp} at 37° C, and figure 1d shows this pattern stabilized by a sweep between 1.85-2.05 MHz and 6 V_{pp} at 1 kHz.

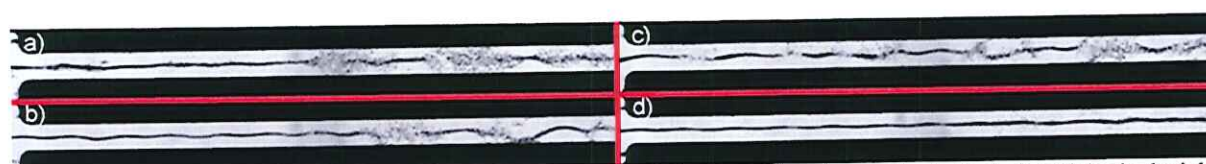


Fig. 2: Stabilization by frequency modulation of two-dimensional alignment (focusing and levitation) of particles in the inlet to the "boxtrap" microcage. The cage is visible in the left edge of the micrographs. Figs. 2a through 2c show single-frequency actuation at 6.90, 6.95 and 7.00 MHz, respectively. The pattern is one of spotwise levitation and spotwise focusing. Fig. 2d shows the effect of sweeping the frequency between 6.90 and 7.00 MHz at 1 kHz, giving focusing and levitation throughout the whole inlet channel.

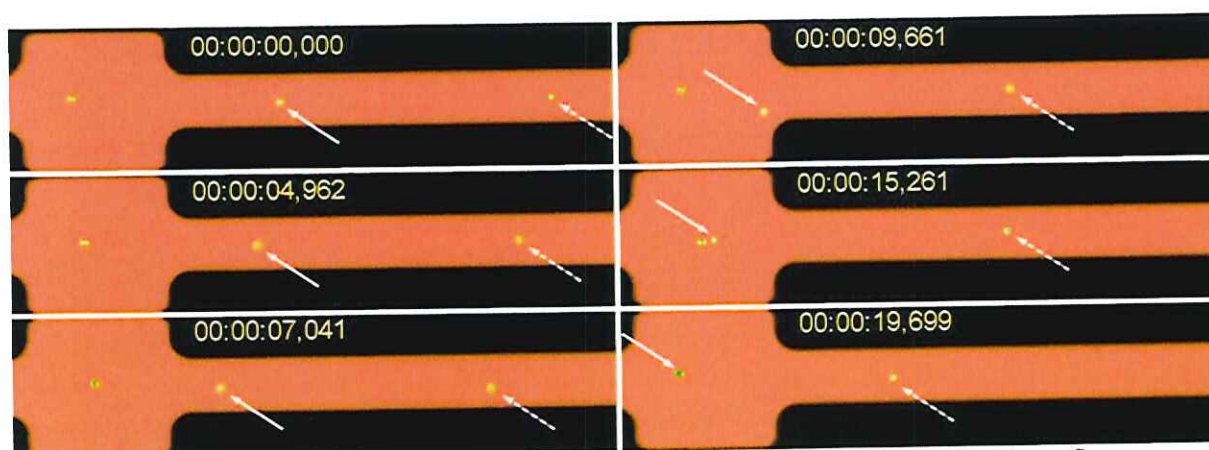


Fig. 3: Time-stamped frames from video showing transportation of 10- μ m polystyrene microbeads under no-flow conditions. The solid and dashed arrows point out two particles as they are transported. Two transducers were used, one sweeping 2.60-2.64 MHz at 0.1 Hz, giving the transportation in the inlet channel and focusing/retention in the cage, and one sweeping 6.90-7.00 MHz at 1 kHz giving the focusing in the inlet and levitation throughout the system (cf. Fig. 2). Both transducers operated at 10 V_{pp} . Several video sequences are available.

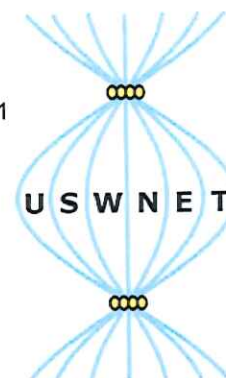
- ¹ J. Hultström et al, "Proliferation and viability of adherent cells manipulated by standing-wave ultrasound in a microfluidic chip", *Ultrasound Med Biol* **33**, 145-151 (2007)
- ² J. Svennebring et al, "Temperature regulation during ultrasonic manipulation for long-term cell handling in a microfluidic chip, *J Micromech Microeng* **17**, 2469-2474 (2007)
- ³ O. Manneberg et al, "Wedge transducer design for two-dimensional ultrasonic manipulation in a microfluidic chip", accepted for publication in *J Micromech Microeng* (2008)
- ⁴ S. M. Hagsäter et al, "Acoustic resonances in straight microchannels: Beyond the 1D-approximation", *Lab Chip* **8**, 1178-1184 (2008)
- ⁵ O. Manneberg et al, "Spatial confinement of ultrasonic force fields in microfluidic channels", in press, *Ultrasonics*, DOI:10.1016/j.ultras.2008.06.012 (2008)
- ⁶ O. Manneberg et al, "A three-dimensional ultrasonic cage for characterization of individual cells", accepted for publication in *Appl Phys Lett* (2008).

Affinity Extraction of Antibodies using Acoustophoresis

Per Augustsson¹, Jonas Persson², Mats Ohlin², Thomas Laurell¹

¹Dept. of Electrical Measurements
Lund University
Lund
Sweden
per.augustsson@elmat.lth.se

²Dept. of Immunotechnology
Lund University
Lund
Sweden



A highly efficient microfluidic particle wash chip was developed for efficient affinity extraction of specific binders from bacteriophage antibody display libraries. Compared to commonplace manual washing procedures this device allows for complete automation of phage display selection, a method with great potential in high-throughput proteomics. The efficiency of the acoustophoretic washing principle was demonstrated by a non-specific phage cross contamination level of only 10^{-6} of that in the input bead and phage mixture.

Phage display

Phage display¹ has become a leading method for isolating new binders from molecular libraries containing large sets of related but different molecules and it is likely to play an extensive role for the development of specific binders, often but not necessarily antibody-type molecules,² against various targets (antigens). Such binders will e.g. allow for assessment of all components of the proteome, an approach important for efficient diagnosis, prediction and treatment of disease. Phage display is normally performed according to the following scheme. The antigen is immobilized to a surface, often in the form of a microbead. Following incubation, phage particles that display antigen-specific antibody fragments will be caught on the antigen-coated surface (Figure 1). By washing away unbound phages, those phages displaying binders targeting the antigen are enriched and they can be used to produce the associated antibody fragments. The procedure of separating rare phages displaying antigen-specific binders from the large bulk of phage particles is a step that needs automation in order to allow isolation of specific binders to all members of proteomes, an effort central to ongoing strategic research consortia³. Current procedures are labouring intense and require manual intervention, preventing high throughput approaches for development of specific binders by this technology.

Acoustophoresis based washing of microparticles

Acoustic particle manipulation has shown great potential for particle washing in micro devices^{4, 5, 6}. The governing force is the acoustic radiation force that is experienced by particles in an acoustic standing wave field. An acoustic standing wave will arise in a silicon/glass microchannel upon actuation of vibrations if the width of the channel is matched to a half wavelength of sound in aqueous medium. Differences in acoustic properties of the particle and the suspending medium make the particle move relative to the fluid in the acoustic field, forming bands of particles in the pressure nodal positions. Particle washing in microchannels can be accomplished by moving the particles acoustically from a contaminated medium near the channel walls into a stream of clear medium in the centre of the channel.

¹ J. McCafferty, A.D. Griffiths, G. Winter, D. Chiswell, *Nature*, 1990, 348, 552-554

² H.K. Binz, P. Amstutz, A. Plückthun, *Nat Biotechnol*, 2005, 23, 1257-1268

³ M. Taussig et al. *Nat. Methods*, 2007, 4, 13-17

⁴ J. J. Hawkes, R. W. Barber, D. R. Emerson and W. T. Coakley, *Lab Chip*, 2004, 4, 446-452

⁵ F. Petersson, A. Nilsson, H. Jönsson and T. Laurell, *Anal. Chem.*, 2005, 77, 1216-1221

⁶ P. Augustsson, L. B. Åberg, A.-M. K. Swärd-Nilsson and T. Laurell, *Microchimica Acta*, 2008, DOI: 10.1007/s00604-008-0084-4

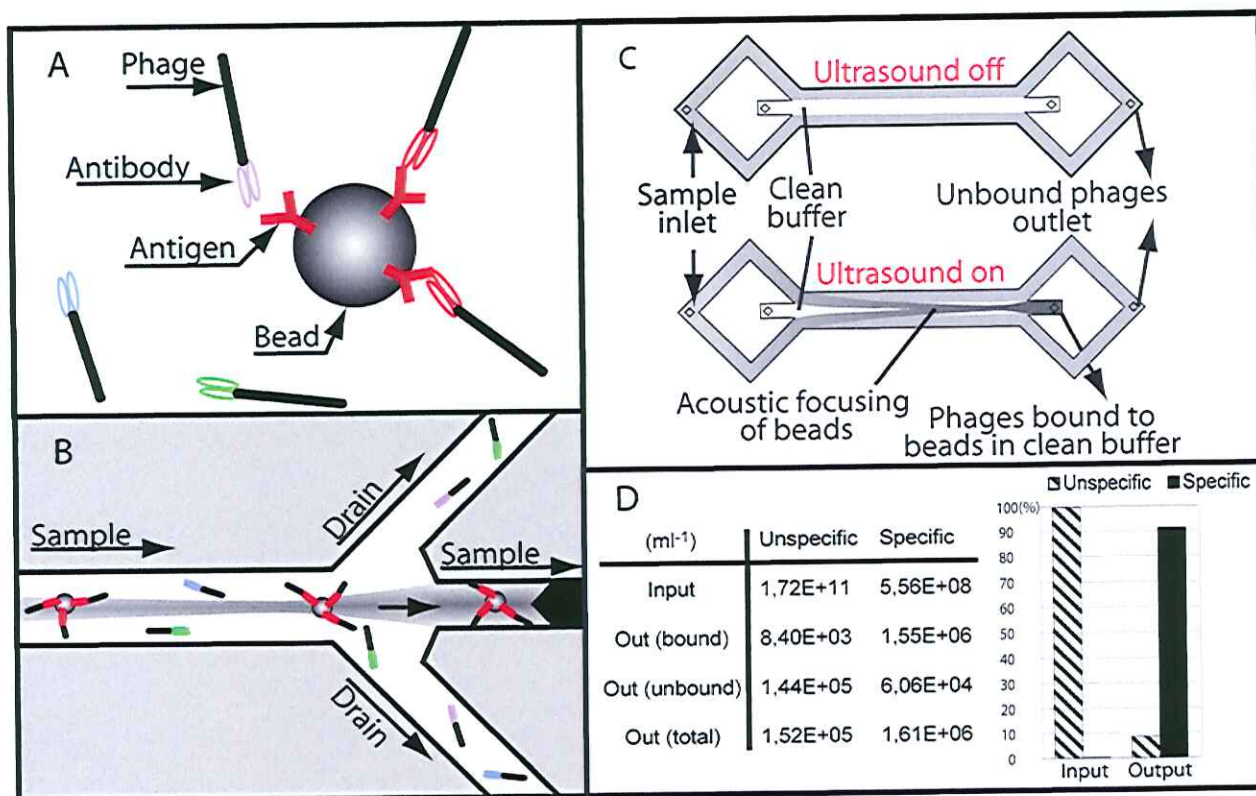


Fig. 1 (A) Principle of phage display selection. Phage particle, displaying a unique protein (encoded by its genome) on its surface, will bind to its cognate antigen, e.g. as coated onto a microbead. Such phages can be separated from other phages not displaying specific binders on their surface. (B) The ultrasound standing wave makes beads focus to the centre of the flow and to exit the separation channel through the central outlet dragging along any specifically bound phages. Non-bound phage particles remain in their flow laminated position along the side of the separation channel and are drained through the side outlets. (C) Principle of operation for a single step acoustic standing wave washing of beads. (D) Diagram showing percent of specific and unspecific phages to the total number of phages in the input and output, respectively. If antigen was present on the beads the specific phage was enriched over 3000 times compared to the unspecific phage.

Experimental and Results

To exploit the primary axial acoustic radiation force in the facilitation of automated phage display selection technology, a chip was developed with the intention of catching phages displaying specific binders and removing the bulk of non-bound phage particles (Fig. 1-2). Phage particles were not by themselves focused by the acoustic radiation force. Rather, they remained in the part of the flow field into which they were injected. In contrast, microparticles could move under the influence of such forces. Phages displaying specific binders were retrieved with the microparticle fraction if their antigen had been immobilized on the bead. In order to achieve high enough washing efficiency, the device performs two sequential cycles of acoustic carrier media particle transfer and washing. This microfluidic design and extensions of it thus has the properties that allow it to be used in automated selection procedures not requiring manual steps involving e.g. centrifugation. The presented two step acoustic extraction of phages displayed thousand fold enrichment of phages displaying specific binders relative to a non specific phage variant (Fig. 1D). We envisage that this technology will provide the basis for automation required to accomplish high throughput selection of specific binders by the state-of-the-art phage display technology.

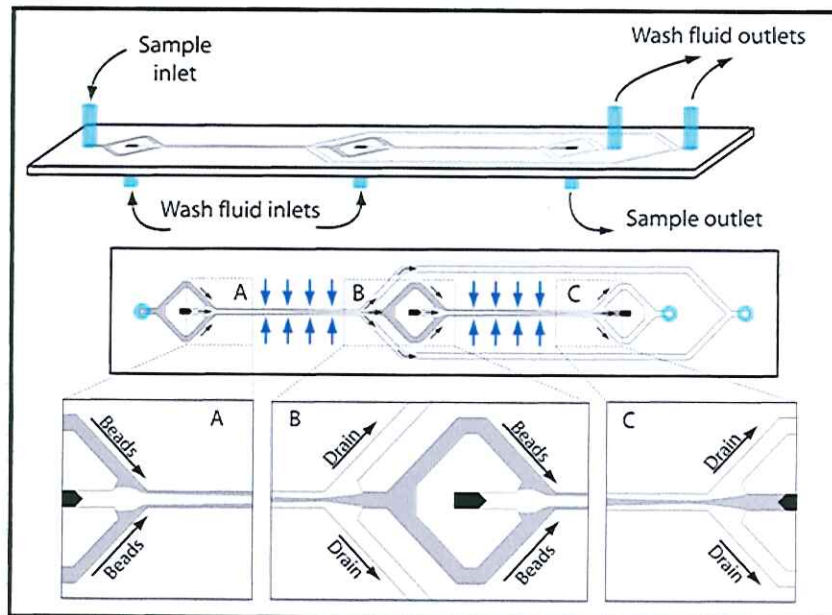


Fig. 2 (Upper) Side view of the particle washing device showing the fluid connections. (Lower) Two narrow streams of sample are injected through the side inlets at A, separated by a stream of fresh wash fluid in the centre of the channel. The beads with the bound species are acoustically focused towards the centre of the channel A-B while bulk of non specific material will remain in the laminar flow path near the channel walls. At B the flow is split up into two drain outlets and a structure for passing along the focused beads to yet another wash step. The beads are again focused into fresh wash fluid between B and C and finally exit the channel through the central outlet.

Conclusions

The presented continuous flow chip constitutes a drastic improvement of acoustophoresis based microfluidic devices for washing of microparticles regarding washing efficiency. Carry-over of non-specific material in the ppm regime relative to input levels makes acoustophoresis suitable for bead based affinity extraction of rare species from complex biofluids, applications that require high purification yield in order to suppress the large background of non specific material.

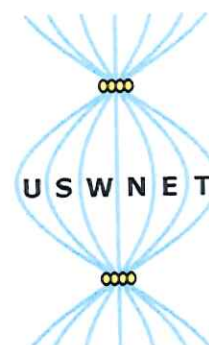
Fractionation of microparticles with acousto-optically generated potential energy landscapes

Michael P MacDonald¹, Graham Milne², Kishan Dholakia³

¹Electronic Engineering and Physics
University of Dundee
Nethergate
Dundee DD1 4HN
Scotland
m.p.macdonald@dundee.ac.uk

²Dept. of Chemistry
University of Washington
Seattle WA 98195-1700
US

³School of Physics and Astronomy
University of St Andrews
North Haugh
St Andrews
Fife, KY16 9SS
Scotland



In an analogous manner to the manipulation of microparticles in ultrasonic standing waves, microparticle motion can be controlled using the periodic optical potential energy landscapes formed by optical patterns. Using such landscapes it is possible to create tailored potentials that lead, in the presence of an external driving force, to particle separation as a result of differences in size, shape or refractive index.

Fractionation according to particle size

In contrast to recent methods of holographic or interferometric generation of such landscapes¹, we use an acousto-optic deflector to create two-dimensional landscapes². This approach allows arbitrary two-dimensional patterns to be formed such that a flexible approach to particle fractionation is possible. Figure 1 shows the particle tracking data for a polydisperse flow of 3 different sizes of colloidal particles (diameters: purple 5.08 μm , green 3.01 μm and blue 2.47 μm). Up to 4 different particle sizes have been separated in this fashion, however there is no fundamental limit to the number of fractionations that can be separated and the system could certainly be extended up to parallel fractionation of as many as 10 different particle sizes.

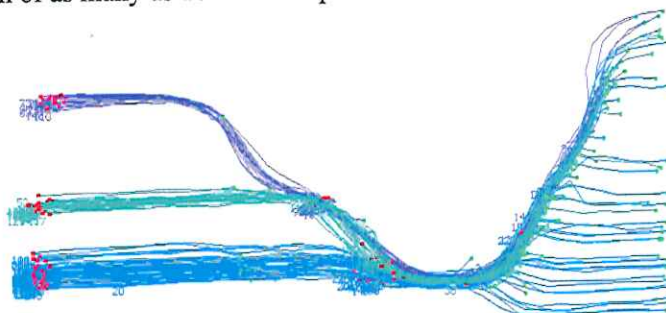


Fig. 1 Parallel fractionation of three different sizes of particles into independent streams. Flow is from right to left. Total height of the image is approximately 20 microns.

Fractionation according to particle shape (blood fractionation)

This method for fractionating microparticles is also sensitive to particle shape, allowing it to be used to filter blood, with the bi-concave disks of erythrocytes being separated from the more spherical lymphocytes. Hence we can obtain continuous separation of blood fractions in a lab-on-a-chip environment without the need for any form of pre-treatment or labelling of the cells.

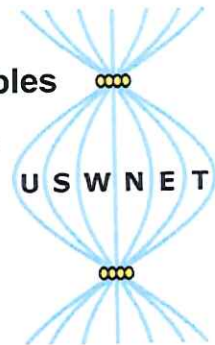
1. MacDonald, M. P., Spalding, G. C. & Dholakia, K. Microfluidic sorting in an optical lattice. *Nature* **426**, 421-426 (2003).
2. Milne, G., Rhodes, D., MacDonald, M. & Dholakia, K. Fractionation of polydisperse colloid with acousto-optically generated potential energy landscapes. *Optics Letters* **32**, 1144-1146 (2007).

Changes of Bubble Dynamics revealed through Optical Micromanipulation of Ultrasound Contrast Agent Microbubbles

Valeria Garbin¹, Nico de Jong^{1,2}, Detlef Lohse¹, Michel Versluis¹

¹Physics of Fluids Group
Dept. of Science and Technology
University of Twente
P.O. Box 217
7500 AE Enschede
The Netherlands
m.versluis@utwente.nl

²Experimental Echocardiography
Biomedical Engineering Group
Erasmus Medical Center
Rotterdam
The Netherlands



Micron-sized gas bubbles are injected in the blood stream to enhance the image quality in ultrasound medical imaging. A full understanding of the interaction of contrast microbubbles with ultrasound, its associated bubble dynamics and the resulting non-linear scattering echoes is important for the optimization of diagnostic imaging protocols. Here we study bubble-wall interactions which are important for molecular imaging applications, where specific binding of targeted bubbles is employed through functionalized coating of the microbubbles to detect disease on a molecular level. We use Laguerre-Gaussian optical tweezers to trap and control the position of single microbubbles and study the interaction with a neighbouring rigid or compliant wall. We optically record the bubble dynamics using an ultra-high speed camera at 15 million frames per second. Acoustical radiation forces are employed to enhance binding of the coated microbubbles to the vasculature. The use of acoustical radiation force leads to a mutual attraction between bubbles due to the secondary Bjerknes force. Here we isolate and position a bubble pair using the optical tweezers and study their complex interaction. The combined setup enabled us to observe purely the effect of the acoustic coupling and it revealed that the attracting bubbles undergo translatory oscillations around a position that is slowly drifting. To account for this effect, in our model we included the viscous drag in the form of Stokes' solution for an oscillating sphere coupled to a history force effect and found good agreement with the experimental data.

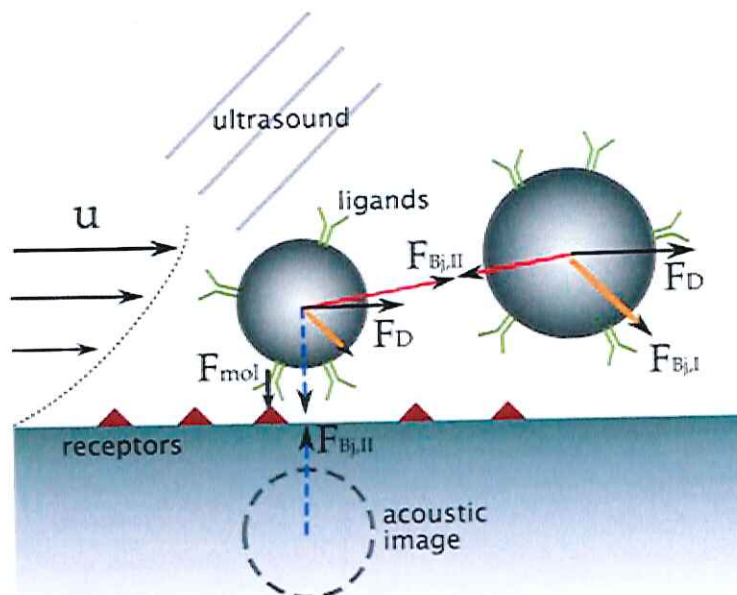


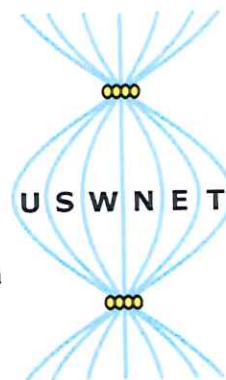
Fig. 1 Diagram showing the fluid mechanical and acoustical forces acting on functionalized microbubbles used for targeted molecular imaging in ultrasound. A set of Laguerre-Gaussian optical tweezers combined with ultra high-speed imaging at the nanoseconds timescale reveals the mutual interaction of bubbles with each other and with the neighbouring wall.

Electrothermal and Electroosmotic Fluid Flow Induced in a Dielectrophoretic Deposition Device

Brian R. Burg¹, Vincenzo Bianco², Julian Schneider¹,
Timo Schwamb¹, Niklas C. Schirmer¹, and Dimos Poulikakos¹

¹Lab. of Thermodynamics in Emerging Technologies
Dept. of Mechanical and Process Engineering
ETH Zurich
8092 Zurich
Switzerland
bburg@ethz.ch

²Dipartimento di Ingegneria Aerospaziale e Meccanica
Seconda Università degli Studi di Napoli
81031 Aversa (CE)
Italy



Strong inhomogeneous ac electric fields, required to produce sufficient force to move a particle in a dielectrophoresis (DEP)-based deposition device, are the origin of thermal gradients, which give rise to electrothermal fluid motion. By superimposing a dc electric field, an electroosmotic flow is generated in the aqueous particle dispersion¹. The influence and interaction of both effects on microfabricated electrode structures is investigated.

Surfactant stabilized single-walled carbon nanotube (SWNT) solutions are used as particle containing fluid medium², enabling individual tube deposition between pre-fabricated electrode gaps. Capacitive coupling of the counter electrode by means of an insulating oxide layer above a conductive substrate, allows the large-scale integration of SWNT networks³.

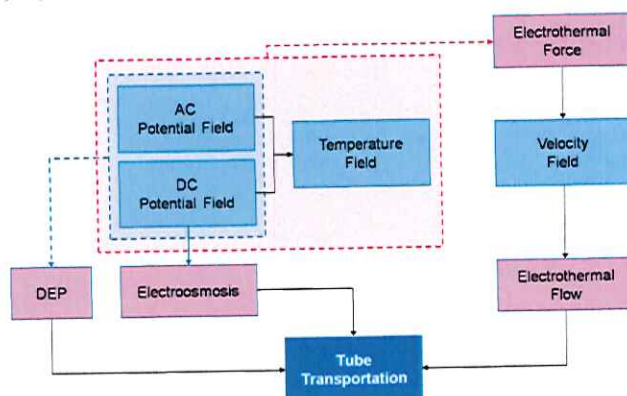


Fig. 1 Electrothermal and Electroosmotic Fluid Flow Interaction

The fluid flow during the dielectrophoretic deposition process is numerically solved, coupling electrical, thermal and fluid mechanical equations. Induced electrothermal flow causes a vortex above the electrode gap, trapping large amounts of particles intended to deposit across the electrodes. When adding a dc potential offset, the resulting tangential fluid flow above the electrodes extracts the particles from the vortex and directs them downwards to the electrode gap, thus increasing the deposition success.

Consequently, a higher deposition yield at overall lower electric field strengths is achieved. Further, the capacitive coupling scheme allows the large-scale parallel deposition of nanostructure networks, without direct current throughput. Overall gentler particle handling is the result, an important aspect for limiting processing influences during device fabrication.

¹H. Morgan, N.G. Green, "Ac Electrokinesis: Colloids and Nanoparticles," Research Studies Press (2003).

²M.J. O'Connell, S.M. Bachilo, C.B. Huffman, V.C. Moore, M.S. Strano, E.H. Haroz, K.L. Rialon, P.J. Boul, W.H. Noon, C. Kittrell, J. Ma, R.H. Hauge, R.B. Weisman, R.E. Smalley, "Band Gap Fluorescence from Individual Single-Walled Carbon Nanotubes," Science 297, 593-596 (2002).

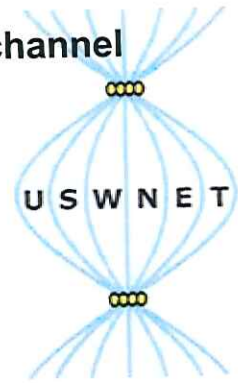
³R. Krupke, F. Hennrich, H.B. Weber, M.M. Kappes, H.v. Löhneysen, "Simultaneous Deposition of Metallic Bundles of Single-walled Carbon Nanotubes Using Ac-dielectrophoresis," Nano Lett. 3, 8, 1019-1023 (2003).

Experimental study of particle motion within a microchannel narrower than half a wavelength

Icíar González¹, Tomás Gómez¹, Luis Fernández²

¹Institute of Acoustics
Dept. of Signals, systems and Ultrasonic technologies
CSIC
Serrano 144, 28006 Madrid
Spain
iacgg38@ia.cetef.csic.es

²Dept. of Mechanical Eng.
IKERLAN
Mondragón
SPAIN



A new device working as a multilayer actuator has been developed for particle manipulation. In it, a standing wave is established across the consecutive layers, with a node of pressure strategically located within the channel.

The present design, unlike other conventional half-wavelength ($\lambda/2$) or quarter/wavelength ($\lambda/4$) ultrasonic resonators, permits that the thickness of some of the layers of the device take values different than the conventional one of multiple quantity of $\lambda/4$. In particular, the width of the channel is narrower than $\lambda/2$ and wider than $\lambda/4$, which does not fit any of the conventional models, but it represents an intermediate situation.

However, a suitable combination of the subsequent layer widths allows the establishment of a standing wave across them that, working in a multilayer mode, generate a node of pressure strategically located within the channel.

In addition, slight variations of the acoustic frequency around that one of resonance of the piezoceramic transducer, generate controlled displacements of the node within the channel.

Figure 1 shows a schematic view of the device. A standing wave is strategically applied on a channel conducted on a chip (layers 3 and 5) to drive the selected particles toward zones of pressure balance inside the channel. A piezoelectric ceramic plate poled in the thickness direction is attached by a thin glue layer (2) to a carrier layer (layer 3). Driven by a conventional generator, this produces the establishment of a complex acoustic field across the width of the channel, perpendicular to its length.

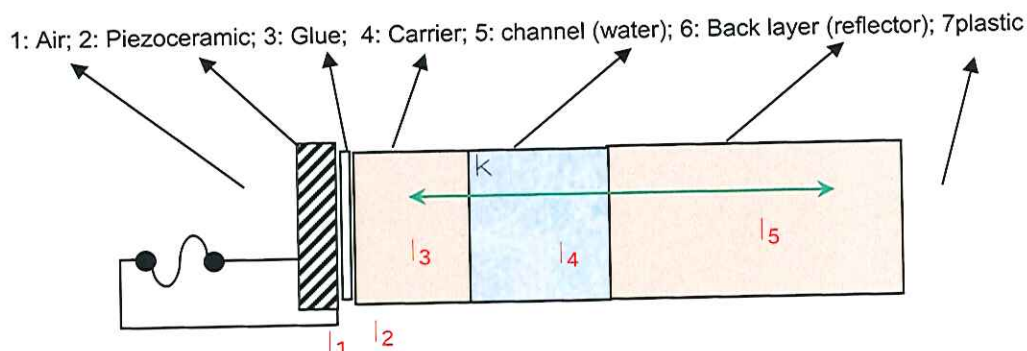


Fig. 1 Schematic view of the multilayer device

In all the experiments the particles (polystyrene beads with diameters of $20\mu\text{m}$) immersed in de-ionized water were filmed during their drift motion due to the axial radiation force within the channel toward the node of pressure, where remained collected during the application of the acoustic field.

Both, reflector and carrier layers were made of a soft material with a low acoustic impedance, not far from that of the water. Although this feature seemed to be less suitable for the production of a resonant cavity, this has the advantage of relaxing the tuning requirements of the resonances of all layers in the device to the same frequency and of reinforcing the generation of resonant modes related to in-phase displacements of the whole multilayered structure. In addition, (as the experimental results confirm) the level of the energy entrapped within the channel is enough to establish a resonant field and to drift the 20 μm polystyrene beads), and the location of acoustic balance is obtained easily within the channel at a selected location.

To know the influence of the carrier layer (layer 3) on the particle motion within the channel, two sets of experiments were conducted for two different designs of the device, that included values of $l_3 = \lambda_3/4$ and $l_3 = 3\lambda_3/8$ (a 10% additional) respectively at the frequency of 1 MHz (resonance frequency of the piezoceramic).

In both cases similar results of the particle behaviour were found, evidencing that the carrier layer was not critical for the spatial distribution of the particle motion in this type of multilayer devices.

On the contrary, any slight variation of the acoustic frequency in a range of approximately 10% around the central frequency produced displacements of the node of pressure within the channel across its width, and, so on, of the particle drift motion, as shown in three filmed images of Figure 2, taken at three frequencies, varying in a range between 930kHz and 1070kHz.

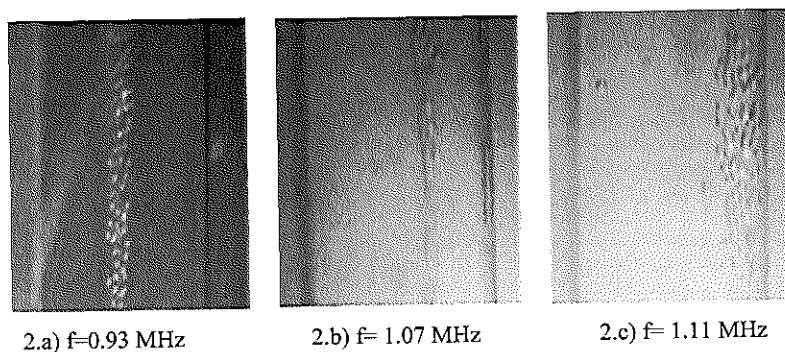


Fig. 2 Different locations of the node of pressure inside the channel where the particles are collected at three different frequencies close to that of the piezoelectric ceramic resonance (1.01 MHz)

In parallel to the experiments, a numerical multilayer simulation was modelled using MATLAB to analyse the influence of each layer on the spatial distribution of the acoustic wave and, with it, on the location of the node of pressure. The width of the reflector layer was found to be determinant on the particle drift motion inside the channel. In the same way, any slight deviation of the frequency generated displacements of the node of pressure within it.

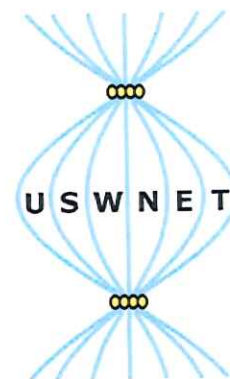
The probed feasibility of this ultrasonic device for the particle manipulation opens the possibility of new technological developments apparently not in conformity with conventional acoustic requirements, allowing the use of new materials acoustically soft and/or combining different sizes of the multilayer elements to achieve strategic locations of particle collection within the channel of treatment, depending on each application.

Towards a Binary Particle Fractionator

Nick Harris, Rosemary Townsend, Martyn Hill

¹School of Electronics and Computer Science
University of Southampton
Highfield
Southampton
SO17 1BJ
nrh@ecs.soton.ac.uk

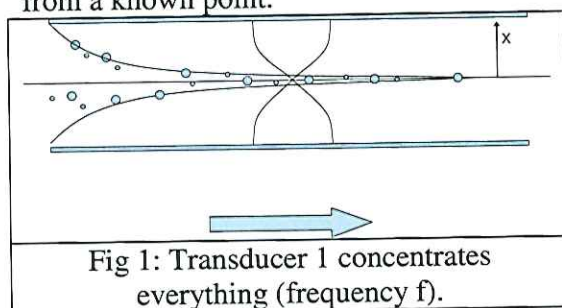
¹School of Engineering Science
University of Southampton
Highfield
Southampton
SO17 1BJ



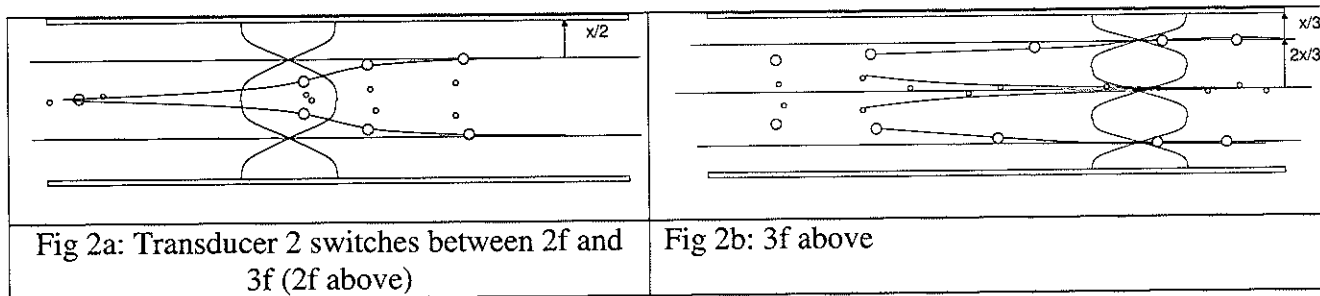
An interesting development towards a robust particle fractionator is presented. Typically acoustic fractionators rely on time of flight in a constant acoustic field to separate different populations[1,2]. Such a system requires all particles to be concentrated to an initial known point before entering the acoustic field. As the particle population enters the acoustic field, the particles will move towards the nodal point at velocities dictated by their relative size. If the size of the acoustic chamber, flow rates and radiation forces are carefully adjusted, particles can be graded across the width of the chamber when they exit the acoustic field.

One potential way of reducing the constraints of this multiple balance is to use frequency switching to reduce the constraint of residence time. In the system described above, an excess dwell time in the acoustic field results in all particles moving to the nodal point. By electronically switching frequencies at a controlled rate, there is no longer a constraint on maximum dwell time. Such a technique no longer allows a continuous grading of the particle sizes across the width of the device, but rather splits the population into 2 fractions, with the split point (in terms of size) being dictated by the frequency switching rate (easily controlled electronically). Such a principle has been demonstrated by Petersson [3], although the technique described here is subtly different from Petersson's technique and will result in relatively narrow bands of particles with clear spatial separation between populations, as once the larger particles have been moved to position, they will tend to move between different nodal planes from the smaller particles. In addition, prefocussing to the centre acoustically avoids the need for sheath flow – an important consideration if the populations are at low concentration or for remote sensing.

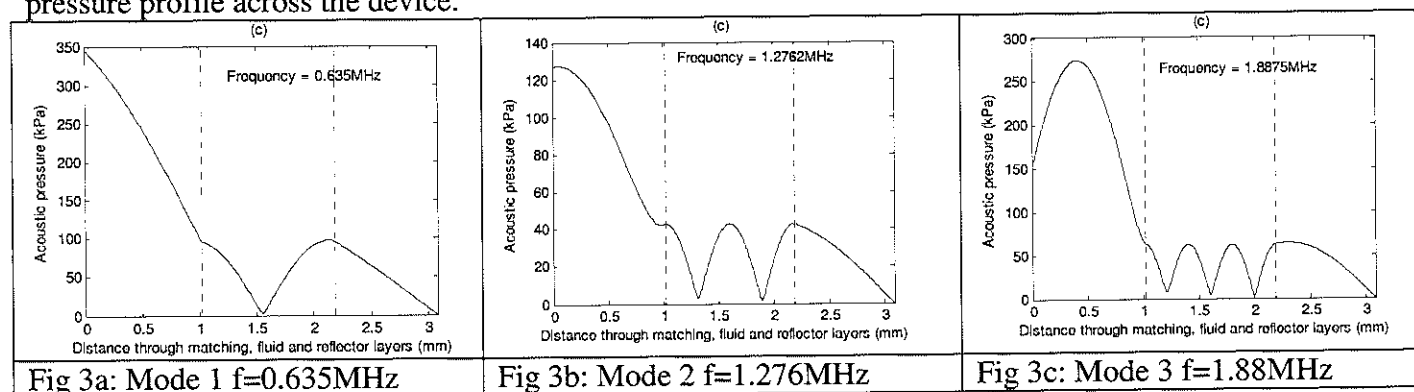
The principle is illustrated below in figures 1 and 2. A chamber with two transducers is used. The first transducer allows all particles to be concentrated into the centre of the chamber, so everything starts from a known point.



The second transducer then applies a switch between two modes to provide the separating mechanism. In this case we are using frequencies of f , $2f$ and $3f$. The effective result of this is that the centre node is periodically removed where two outer modes are maintained. Thus larger particles that move faster will reach the outer nodes whereas smaller particles are pulled back to the centre.

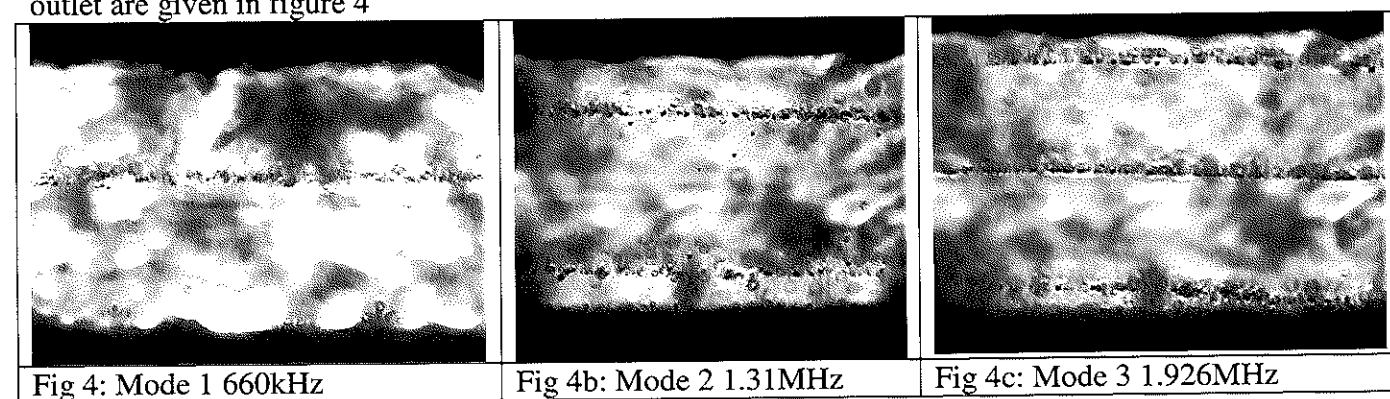


Modelling of a multilayer structure based on the principles used in [4] enabled a design that could efficiently support all three modes described above to be evaluated. Figure 3 shows the predicted pressure profile across the device.



The device was constructed from brass with a glass reflector layer to allow visibility into the device. The resonances of the device were established to be at 660kHz, 1.31MHz and 1.926MHz, in good agreement with the model.

Testing with particles was carried out to confirm the activity of the modes, and images from the outlet are given in figure 4



In each case the particles illustrate the location of the nodes.

References

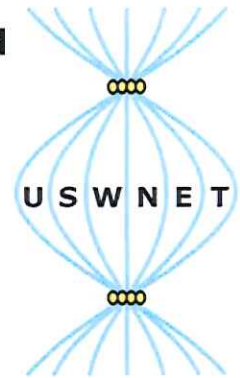
- Petersson, F., et al., *Free Flow Acoustophoresis: Microfluidic-Based Mode of Particle and Cell Separation*. Anal. Chem., 2007. **79**(14): p. 5117-5123.
- Kumar, M., D.L. Feke, and J.M. Belovich, *Fractionation of cell mixtures using acoustic and laminar flow fields*. Biotechnology And Bioengineering, 2005. **89**(2): p. 129-137.
- Petersson, F., *On Acoustic Particle and Cell Manipulation in Microfluid Systems*, PhD Thesis, Department of Electrical Measurements. 2007, Lund University: Lund. p. 51-52.
- Harris, N.R., et al., *A dual frequency, ultrasonic, microengineered particle manipulator*. Ultrasonics, 2004. **42**: p. 139-44.

Two dimensional acoustic standing wave fields in open and closed systems

Stefano Oberti¹, Adrian Neild², Jurg Dual¹

¹Institute of Mechanical Systems
Dept. of Mechanical and Process Eng.
ETH Zurich
CH-8092 Zurich
Switzerland
stefano.oberti@imes.mavt.ethz.ch

²Dept. of Mechanical Eng.
Monash University
Melbourne
Australia



Introduction

In *micro total analysis* systems the physical handling of micron sized particles (e.g. coated beads, cells) is often a necessary step in addition to the actual biochemical analysis. The use of acoustic forces has revealed itself to be a valid solution. Most acoustic devices are operated in flow-through mode [1-3], where suspended particles are concentrated into parallel planes in one dimensional standing pressure fields while they are flowing down a channel. Some applications, however, require operation in batch mode. For instance, when prolonged observation of the sample or when drug screening has to be performed, particles or cells need to be trapped at specific locations. On the other hand, in the field of planar microfluidics, once a chemical reaction has taken place by mixing the fluid with suspended coated beads, these could be extracted from the fluid by concentrating them in the middle of a droplet and then removed by means of a pipette or through an orifice. Both of these applications require two dimensional positioning of the sample itself (assuming the sample sits on the bottom of a channel in the third direction).

Method

The excitation of two dimensional acoustic fields relies on constraints set by the fluidic cavity geometry or on the superposition of fields acting in different directions. In the case of a rectangular chamber, resonances are set up in each direction at different frequencies and hence full plate actuation using the sum of two signals would suffice to gather suspended particles into circular clumps at the intersection of the lines that would be formed by the one dimensional standing pressure fields. However, it is preferable to have a method which is independent of the cavity geometry, and which can be applied for instance to a square chamber. This can be achieved by having displacement fields in the solid structure containing the fluid cavity, which couple to the fluid in different directions. A method to do this consists in the use of different transducers [4] to excite resonances in different directions. Another method is discussed here, which is based on the excitation of displacement fields on the same piezoelectric plate, by the activation of different areas, defined on the transducer surface in form of stripes. This method is particularly suited for systems of reduced size [5], as it permits to have the actuation exactly where needed, by keeping the heat generation at low level.

Results

The piezoelectric transducers can be operated to produce desired pressure fields in the fluid. Here we complete the set of strategies described previously [6] with the addition of a new one, in which the electrodes are excited individually but alternately. As the force fields resulting from each electrode are not created concurrently, the resulting overall force field can be found by a further time average of these two individual force fields. Hence the particles will be collected at the areas in which both force fields have potential minima, or rather as close to that as possible given volumetric restraints. This method has been used for the creation of two dimensional arrays in a

rectangular chamber (5 x 5.9 x 0.2 mm). At 2210 kHz (z -direction) and 2750 kHz (x -direction), respectively, both one dimensional standing pressure fields have the same wavelength and hence the lines intersect in a regular square grid when switching is done.

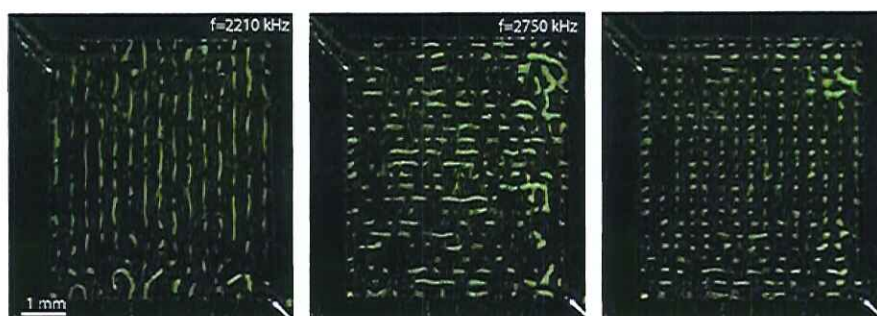


Fig. 1 Creation of two dimensional patterns in a rectangular chamber by the alternate excitation of two orthogonally oriented electrodes at different frequencies. The first two pictures show the one dimensional standing pressure fields, whereas the third one depicts the resulting two dimensional pattern when switching is performed.

Furthermore, this method has been used for the concentration of 16 μm particles at the centre of a droplet (diameter 3 mm) deposited on a glass surface excited by a piezoelectric transducer located beneath it [7]. Firstly the electrode which runs along the horizontal axis of the image is activated, and a line formed (a), then the signal is switched to the orthogonal electrode and a line is formed approximately parallel to the vertical axis of the image (b) already this line is shorter than the first formed. The switching is repeated twice more, in order to form a clump of particles at the centre of the droplet (d).

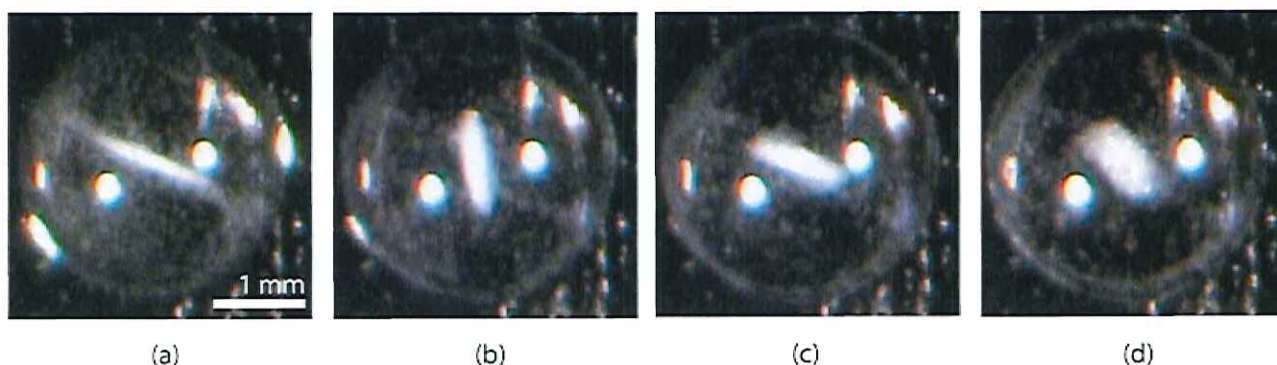


Fig. 2 Concentration process of 16 μm particles in a droplet by alternatively exciting single electrodes. Particles align approximately parallel to the excited electrode. It can be seen in moving from (a) to (b) that the particles in the broad ends of the line are pulled into the centre of the droplet when the switch occurs, hence a higher proportion of the particles are held in this single location. The two bright dots are the reflections of the lamp on the droplet surface

Conclusions

Different strategies for the excitation of two dimensional pressure fields by the use of a single transducer have been reviewed here and their application on different systems has been shown.

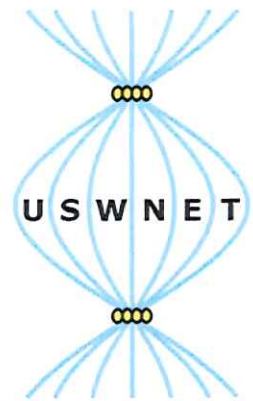
- [1] T. Laurell, F Petersson and A Nilsson, *Chem. Soc. Rev.*, 36 (2007), pp. 492-506
- [2] N. Harris, M. Hill, Y. Shen, R.J. Townsend, S. Beeby, N.M. White, *Ultrasonics*, 42 (2004) pp. 139-144
- [3] M. Wiklund, C. Günther, R. Lemor, M. Jäger, G. Fuhr and H. M. Hertz, *Lab chip*, 6 (2006) pp. 1537-1544
- [4] O. Manneberg, J. Svennebring, H.M. Hertz, M. Wiklund, *J. Micromech. Microeng.*, 18 (2008) pp. 1-9
- [5] S. Oberti, A. Neild, D. Möller, J. Dual, *Ultrasonics* (2008), in press (doi: 10.1016/j.ultras.2008.06.004)
- [6] S. Oberti, A. Neild, J. Dual, *J. Acoust. Soc. Am.*, 121 (2007), pp. 778-785
- [7] S. Oberti, A. Neild, R. Quach, J. Dual, *Ultrasonics* (2008), in press (doi: 10.1016/j.ultras.2008.05.002)

Single-particle control by electric fields: from living cells to viruses and nanowires

Magnus S. Jaeger¹, Michael Boettcher¹,
Stefan Fiedler², Michael Zwanzig², Claus Duschl¹

¹Fraunhofer Institute for Biomedical Engineering (IBMT)
Am Muehlenberg 13
14476 Potsdam
Germany
magnus.jaeger@ibmt.fraunhofer.de

²Fraunhofer Institute for Reliability and Microintegration (IZM)
G.-Meyer-Allee 25
13355 Berlin
Germany
stefan.fiedler@izm.fraunhofer.de



Motivation

Driven by the boundary conditions that the work with small numbers of living cells imposes, a range of methods has been developed in biotechnology and medicine over the last decades for manipulating individual microparticles. They all have in common that they are based on gradients of fields: light¹, radio-frequency electric fields², magnetic fields, hydrodynamic velocity or pressure³. Considerable steps forward were achieved by combinations of these techniques in one application⁴. Here, we aim at extending the manageable object dimensions down into the nanorange by combinations of two of the above-mentioned principles: on the one hand the simultaneous action of flow fields and electric fields⁵, and on the other hand employing electric fields together with ultrasound⁶.

Principles

Objects that differ in their polarisability from the surrounding medium experience a force in an inhomogeneous electric field. This results from the interaction between the generating field itself and the effective dipole induced in the particle⁷. Sophisticated set-ups based on this principle serve to identify, sort, characterise and fuse individual living cells. They consist of fluidic systems with integrated microelectrodes⁸. In addition, these forces may also be exerted on portions of the fluid volume if the dielectric material properties of the liquid vary spatially⁹. Analogous to the situation on particulate suspensions, such inhomogeneities can be created through the action of the electric field itself. In consequence, this leads to the occurrence of a fluid flow.

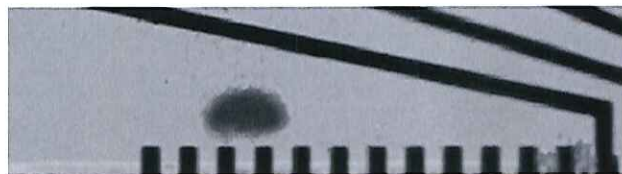


Fig. 1 An aggregate of 1 μm diameter suspended particles formed by a register of 10 μm wide microelectrodes (black patches).

Results

Under suitable dielectrophoretic conditions, linear arrays of parallel microelectrodes exert a directed force on the fluid in a microchannel, thus causing a pumping. However, stationary vortices occur at the boundaries of the arrays. Suspended particles in the fluid experience a combined hydrodynamic and dielectrophoretic effect. Interestingly, this leads to a particle accumulation and the formation of stable clusters at defined positions in the chip. As we could show, this continuous filtering of objects from a flowing liquid is effective for particles down to 200 nm in diameter and still measurable in 50 nm parti-

cles. The underlying aim is to employ this principle in an improved detection of viral particles. Additionally, it could be put to use for investigating processes during viral infection on a single-cell level.

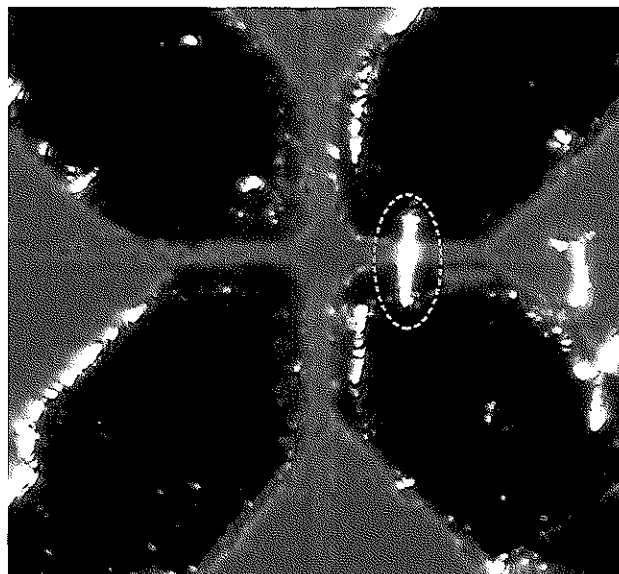


Fig. 2 Manipulation of individual gold nanowires (thickness 600 nm) by means of dielectrophoretic forces. One nanowire (broken line) has been positioned so as to connect the two rightmost of the four microelectrodes.

Another line of our research concerns transferring single-particle manipulation methods originally devised for biomedical applications to assembly and packaging in microelectronics. The perpetual challenge posed by circuit miniaturisation requires novel processing methods. Since comparable problems have already been solved in the biological field, approaches like handling by dielectrophoresis or ultrasonic standing waves lend themselves naturally to being translated into the manipulation of functional nanoelements. Examples for the latter are metal wires made from gold or nickel (thickness about 600 nm) and quantum dots (diameter about 20 nm).

¹ C. Reichle, T. Schnelle, T. Mueller, T. Leya, G. Fuhr, "A new microsystem for automated electrorotation measurements using laser tweezers," *BBA* **1459**, 218-229 (2000)

² T. Mueller, A. Pfennig, P. Klein, G. Gradl, M. S. Jaeger, T. Schnelle, "The Potential of Dielectrophoresis for Single-Cell Experiments," *IEEE Eng Med Biol* **22**, 51-61 (2003)

³ J. Hultstrom, O. Manneberg, K. Dopf, H. M. Hertz, H. Brismar, M. Wiklund, "Proliferation and viability of adherent cells manipulated by standing-wave ultrasound in a microfluidic chip," *Ultrasound Med Biol* **33**(1), 145-151 (2007)

⁴ C. Reichle, K. Sparbier, T. Mueller, T. Schnelle, P. Walden, G. Fuhr, "Combined laser tweezers and dielectric field cage for the analysis of receptor-ligand interactions on single cells," *Electrophoresis* **22**, 272-282 (2001)

⁵ M. Felten, P. Geggier, M. Jaeger, C. Duschl, "Controlling electrohydrodynamic pumping in microchannels through defined temperature fields," *Phys Fluids* **18**, 051707 (2006)

⁶ M. Wiklund, C. Guenther, R. Lemor, M. Jaeger, G. Fuhr, H. M. Hertz, "Ultrasonic standing wave manipulation technology integrated into a dielectrophoretic chip," *Lab Chip* **6**, 1537-1544 (2006)

⁷ A. Ramos, H. Morgan, N. G. Green, A. Castellanos, "AC electrokinetics: a review of forces in microelectrode structures," *J. Phys. D: Appl. Phys.* **31**, 2338-2353 (1998)

⁸ S. Fiedler, R. Hagedorn, T. Schnelle, E. Richter, B. Wagner, and G. Fuhr, "Diffusional Electrotitration: Generation of pH Gradients over Arrays of Ultramicroelectrodes Detected by Fluorescence," *Anal Chem* **67**, 820-828 (1995)

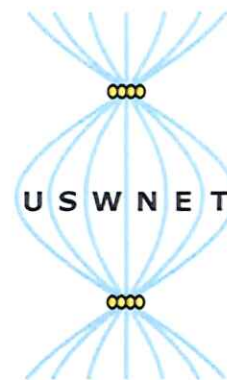
⁹ T. Mueller, W. M. Arnold, T. Schnelle, R. Hagedorn, G. Fuhr, U. Zimmermann, "A traveling-wave micropump for aqueous solutions: Comparison of 1 g and μ g results," *Electrophoresis* **14**, 764-772 (1993)

Infrared absorbance spectra of water influenced by an ultrasonic standing wave

Stefan Radel¹, Markus Brandstetter², Bernhard Lendl¹

¹Institute Chemical Technologies and Analytics
Vienna University of Technology
Getreidemarkt 9/164
A-1060 Wien
Austria
stefan.radel@tuwien.ac.at

²Institute of General Physics
Working group sensors and ultrasound
Vienna University of Technology
Wiedner Hauptstraße 8-10/134
A-1040 Vienna
Austria



The ATR (Attenuated Total Reflection) spectroscopy is a widely used method for infrared (IR) vibrational spectroscopy especially in connection with highly IR absorbing samples like e.g. aqueous solutions. The main advantage of this method is that only a thin film of some micrometers in the proximity of the ATR sensitive element (ATR crystal) is spectroscopically analyzed. Therefore the IR signals of samples suspended in highly absorbing substances reach sufficient values.

The IR sensitive region is defined by the evanescent field, which is caused by total reflection of an IR light beam within the ATR crystal. In other words the light beam isn't really crossing the sample but the field properties of the totally reflected electromagnetical wave and hence the structure of the measured spectrum are influenced by the properties of the substances located within the evanescent field.

When analyzing suspensions by means of ATR spectroscopy one has to bring a sufficient amount of the suspended particles close to the ATR crystal in order to achieve proper absorbance signals. Recently Radel et al.¹ studied the use of an ultrasonic standing wave to enhance the settling of suspended particles on a horizontally placed ATR probe. The underlying principle was the agglomeration by the radiation forces exerted on the particles in suspension. In the beginning the particles were driven towards planes perpendicular to the propagation direction of the ultrasonic field. Subsequently particles were concentrated within the planes by the transversal radiation force². These agglomerations settled faster on the ATR probe than the single particles did.

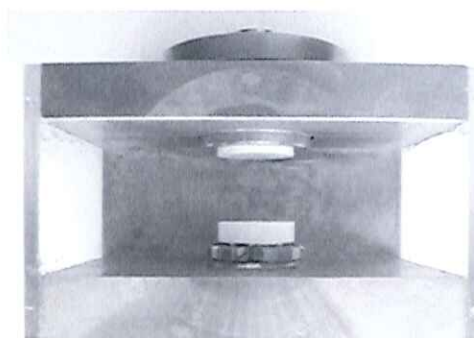


Fig. 1 Picture of the brass cell after the measurements. The upper white part is the Macor® carrier plate of the transducer. The lower white part is the Macor® cover of the ATR probe.

¹ Radel, S.; Schnöller J.; Lendl, B.: "Ultrasonic particle manipulation exploited in on-line infrared spectroscopy of (cell) suspensions." *Elektrotechnik & Informationstechnik*, **125**(3), 76-81 (2008)

² M. Gröschl, "Ultrasonic separation of suspended particles – Part I: Fundamentals." *Acustica united with acta acustica*, **84**, 432-447 (1998)

Very often the particles of interest are suspended in water, which certainly has a distinct spectral absorption itself. Changes of this specific absorbance of water brought about by the ultrasonic standing wave when doing ATR measurements bears the danger of misinterpretation of the acquired spectrum

One influence of ultrasound on water very likely is moderate increases of temperature originating from viscous damping, i.e. the conversion of mechanical (acoustical) energy into heat. Temperature changes considerably change the IR absorbance spectra of water³, hence the aim of this study was the investigation of the effects of temperature increase brought about by an ultrasonic standing wave on the infrared spectrum of water. Absorbance spectra were recorded under the presence of an ultrasonic standing wave as well as with temperate water in the range between 23°C and 45°C.

The performed experiments lead to the result that an ultrasonic standing wave affects ATR absorbance measurements of water significantly (see Fig. 2). Especially in the case of high true electrical power input and long term measurements the changes in the absorbance were considerable. The reason for the variations in the spectrum was very likely energy dissipation of the ultrasonic field in water, which lead to a local increase of temperature. This qualitative and quantitative knowledge can be taken into account doing low signal ATR measurements in aqueous solutions.

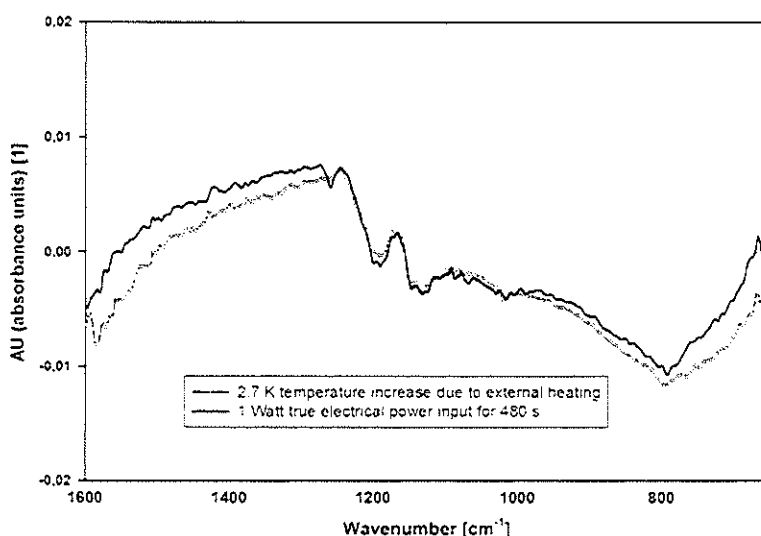


Fig. 2 Comparison of the variations in the absorbance spectra of water due to external heating in absence of an ultrasonic field (solid line) and due to an applied ultrasonic standing wave without external heating (line with dots). Exposure time 480 s at 1 Watt true electrical power input compared with 2.7 K temperature increase (from 23°C to 25.7°C).

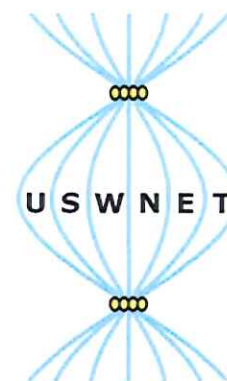
Vice versa, the investigated effect of the ultrasonic standing wave on the absorbance of water bears the potential to indirectly determine the actual temperature in the proximity of the ATR sensitive element by evaluating the variations in the absorbance spectrum. With this knowledge of the local temperature one can then calculate the spatially resolved energy dissipation of the ultrasonic field. By doing so, one could gain additional information in respect to improve theoretical analysis of layered ultrasonic resonators.

³ P. Snoer Jensen, J. Bak, S. Andersson-Engels "Influence of Temperature on Water and Aqueous Glucose Absorption Spectra in the Near- and Mid-Infrared Regions at Physiologically Relevant Temperatures." *Applied Spectroscopy*, 7(1) 28-36 (2003)

Effective mixing of laminar flows at a density interface by an integrated ultrasonic transducer

Linda Johansson¹, Stefan Johansson¹, Fredrik Nikolajeff¹,
Sara Thorslund¹

¹Angström Laboratory
Uppsala University
Uppsala, Sweden
linda.johansson@angstrom.uu.se



ABSTRACT

An acoustic mixer for glass channel microfluidic systems is presented. An acoustic standing wave, perpendicular to the fluid flow, is generated by the excitation of a miniaturized piezoelectric transducer operated around 10 MHz. The mixing occurs at a fluid-fluid density interface due to the acoustic radiation force; an analytical expression is derived to qualitatively describe this phenomenon. Only a density difference in the range of 2-5 % is required to achieve effective peak broadening of a fluorescent sample between sheath flows.

KEYWORDS: Mixing, Density difference, Acoustic, Transducer

INTRODUCTION

Microfluidic systems with channel dimensions from a few microns up to several hundreds of microns possess the property of having complete laminar flows, due to low Reynolds number. Laminar flows are mostly considered advantageous and constitute an important cornerstone within microfluidics, since this makes it possible to predict in a very precise manner where molecules are transported within the system. In the absence of specially designed mixing structures, mixing in these laminar-based flow systems is only accomplished by passive interdiffusion between the fluids. However, many reactions and analyses require well-mixed fluids and to reduce the analysis time of a miniaturized system, the mixing becomes a key unit operation. On-chip applications include e.g. enzyme reactions, cell lysis, immunoassay interactions and hybridization reactions.

The system evaluated here utilizes the acoustic radiation force on an interface between two liquids with different density and this interface is oriented *parallel* to the wave propagation in a standing wave cavity operated around 10 MHz. At this operation frequency, viscous absorption losses in the fluid are small and the frequency enable resonance in the fluid. Resonance in the fluid generates high acoustic amplitudes that are useful in employing acoustic forces in general. The lateral dimensions of the transducer (900*900 μm) enable local activation in a small area of the channel, thereby allowing the handling of small sample volumes with small dead volume.

THEORY

A theoretical description of the radiation force has earlier been presented by Rozenberg,¹ however for a density interface *perpendicular* to the wave propagation direction. In analogy, we have derived an expression for the present system, i.e. where the radiation force acts on an interface *parallel* to the direction of the wave propagation, between liquids of different density. In summery, the maximal radiation force on an interface of fluid 1 and fluid 2 parallel to the wave propagation may be expressed as

$$\left. \frac{F_{r_{1 \rightarrow 2}}}{A} \right|_{\max} = \frac{Q_{SW} \langle p_{a1}^2 \rangle_{\max}}{2\rho_{01}c_{01}^2} - \frac{Q_2 \langle p_{a2}^2 \rangle_{\max}}{2\rho_{02}c_{02}^2} = \frac{\langle v_i^2 \rangle}{2} Q_{SW} \left(\rho_{01} - e^{\frac{-(f_2 - f_{SW})^2}{4 \ln 2}} \rho_{02} \right) \quad (1) \quad (3.7)$$

for the case where the fluid 1 is supporting the standing wave. Q_{SW} is the Q-value supporting the standing wave, p_a the pressure amplitude due to the acoustic field, ρ_0 the density of the medium, c_0 the speed of sound, v_i the velocity at the transducer-fluid interface and f the channel frequency. Viscous forces were ignored for simplicity.

EXPERIMENTAL

A schematic view of the device is shown in Figure 1a and 1b. Miniature single layer PZT-ultrasound transducers, $900 \times 900 \times 200 \mu\text{m}$, were integrated into the bottom channel wall. The channel-reflector structure was fabricated by wet etching borosilicate glass wafers to a reflector thickness of $923 \mu\text{m}$ and $71 \mu\text{m}$ channel depth. The glass-PCB device was sandwiched between two brass plates and pressure sealed by screwing the upper and lower plates tightly together.

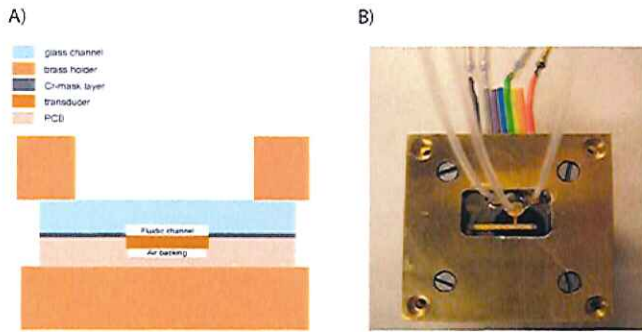


Figure 1. Schematic image and photo of the device having three integrated acoustic transducers for fluid mixing.

RESULTS AND DISCUSSION

A typical intensity profile for a set-up with *lower-density middle flow* and the mid-channel transducer is displayed in Figure 2a. The middle fluid is fluorescently labeled with Rhodamine B. The transducer was run with a driving frequency of 10.3 MHz and the system had a total fluid flow of $3 \mu\text{L min}^{-1}$ (0.7 mm s^{-1}). A mixing sequence above the transducer is shown in Figure 2b with 60 ms between the images, the fluids entering the system from the right. It is evident that the mixing starts from

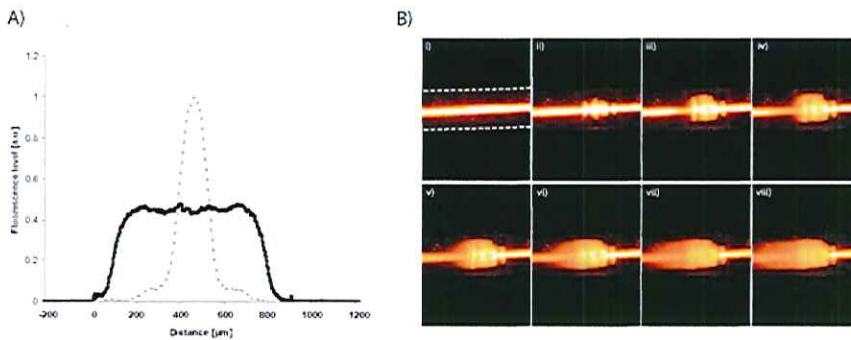


Figure 2. a) The intensity profiles across the fluid channel $500 \mu\text{m}$ downstream the transducer, before (dotted grey) and after (black) transducer activation. (b) A sequence of images of the distribution of the fluorescently labeled middle flow above the mid-channel transducer. The time interval between each image (i-viii) is 60 ms.

the interface surfaces and moves the lower-density fluid into the higher-density fluid, in agreement with the proposed theory, provided that the channel is matched for the lower-density fluid. The fluid convection of the lower-density fluid is fastest at four positions on either interface, Figure 2bii, which corresponds to the spatial pattern of the pressure amplitude in the acoustic near field. At the next stage, Figure 2biii, the fluid moves in the direction normal to the interface created by the initial

mixing movement. The convective motion proceeds until the density difference is equalized, Figure 2bvii. Analyzing the mixing speed at a position 500 μm downstream the transducer, the main part of the mixing, 80%, occurred within 0.36 s and the mixing was completed after additional 0.72 s.

CONCLUSIONS

We present an effective mixing device for microfluidic applications. It is shown that the acoustic radiation force generated by an integrated piezoelectric transducer acts on the fluid density interface parallel to the wave propagation direction. A density difference between the sample and sheath fluids of 4.5 % yields a mixing efficiency of 400 % peak broadening for the case of a lower-density middle flow. For this standing wave mixer, no acoustic streaming was observed. Compared with mixing induced by acoustic streaming it is advantageous that this mixing is not caused by acoustic absorption losses, especially when temperature increase in the channel is critical.

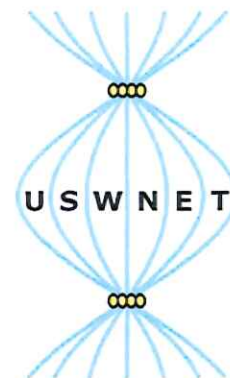
REFERENCES

- [1] L.D. Rozenberg, High-intensity ultrasonic fields; Plenum Press: New York, (1971).

Acoustic streaming at ultrasound resonances in microfluidic chambers: theory and simulation

Peder Skafte-Pedersen and Henrik Bruus

Department of Micro- and Nanotechnology
Technical University of Denmark
DTU Nanotech, Building 345 East
DK-2800 Kongens Lyngby
Denmark
Email: Henrik.Bruus@nanotech.dtu.dk
URL: www.nanotech.dtu.dk/microfluidics



1. Introduction

In a series of recent papers written in collaboration with our experimental colleagues at the Technical University of Denmark (Jörg Kutter's group), at Lund University (Thomas Laurell's group) and at the Royal Institute of Technology (Martin Wiklund's group), we (Henrik Bruus's group) have demonstrated how theoretical analysis and full numerical simulation play an important role for the interpretation of various measurements of acoustic radiation forces and acoustic streaming in microsystems exposed to piezo-induced ultrasound tuned to resonance conditions [1–3].

2. Setup

The typical setup is shown in Figs. 1(a) and (b). A silicon-based microfluidic system, in which a water-filled chamber is connected to in- and outlets and sealed by a glass lid, is placed on top of a piezo crystal. By properly tuning the MHz frequency of the AC-voltage bias applied to the piezo crystal, ultrasonic resonances can be set up in the microchamber. A numerical simulation of the first-order pressure field p_1 at one particular resonance in an arbitrarily shaped micro chamber is shown as the color-scale plot in Fig. 1(c), where also the pressure nodal lines are indicated by thin black lines.

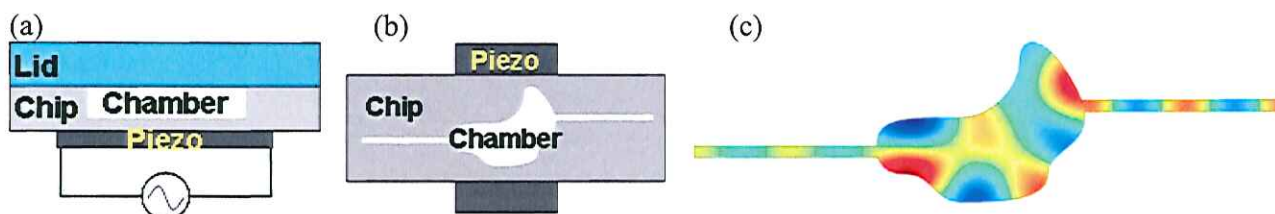


Fig. 1. (a) A side view of the typical setup. A chamber of height $200\ \mu\text{m}$ and a width of approximately $2\ \text{mm}$ is etched into a silicon chip and covered by a glass lid. The device is placed on top of a MHz AC-biased piezo crystal. (b) A top view of the system. (c) A numerical simulation of the pressure field at a particular resonance shown as a color-plot. The pressure nodal lines are represented by the thin, black lines.

3. Governing equations

A basic introduction to the theory of acoustofluidics is given in Ref. [4]. The first-order pressure and velocity fields, p_1 and \mathbf{v}_1 , are found through the Helmholtz equation for the entire system given a time-harmonic excitation $\cos(\omega t)$ modeling the action of the piezo crystal. The small viscous damping is not taken into account in this part of the calculation. The resulting first-order fields then act as sources to the second-order acoustic pressure and velocity fields, p_2 and \mathbf{v}_2 . Due to the inherent non-linearity of the Navier–Stokes equation, the second-order fields have non-zero time averages even for the harmonic temporal first-order excitation. It is these slowly varying time averaged responses that are observed in particle image velocimetry measurements [1].

4. Acoustic streaming and loss of acoustic energy through the chamber walls

Our analysis indicates that the observed acoustic streaming, depicted in Fig. 2(a) adapted from Ref. [1], with its 6×6 vortex pattern, can only be understood in terms of the first-order acoustic pressure and velocity fields, p_1 and \mathbf{v}_1 , shown in Fig. 2(b), if the loss of first-order acoustic radiation energy through the walls of the chamber is taken properly into account, see Figs. 2(c)–(f).

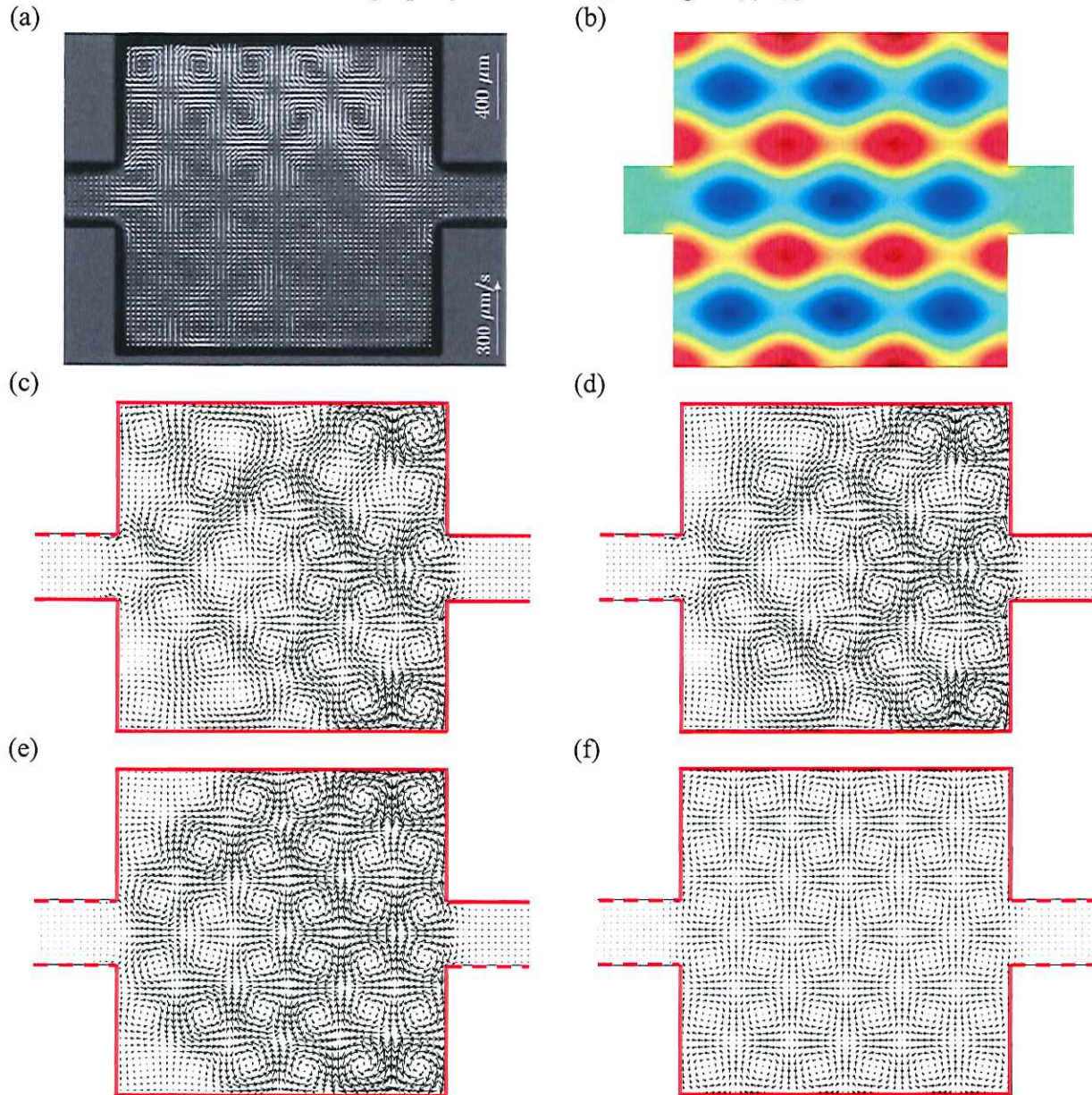


Fig. 2. (a) Acoustic streaming in a $2 \times 2 \times 0.2 \text{ mm}^3$ chamber measured by micro particle image velocimetry, adapted from Ref. [1]. (b) Simulated first-order pressure field p_1 in color scale. (c)–(f) Simulated bulk part $\langle \mathbf{v}_2 \rangle = -\langle p_1 \mathbf{v}_1 \rangle / (\rho_0 c_a^2)$ of the acoustic streaming with various configurations of hard wall boundary conditions (full lines) and lossy acoustic impedance boundary conditions (dashed lines). Note how the asymmetric 6×6 vortex patterns in panel (c)–(e) changes into the symmetric 6×6 vortex pattern in panel (f) as the boundary conditions are changed from being asymmetric to symmetric.

References

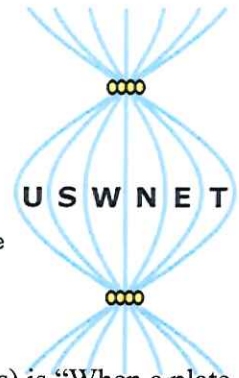
- [1] S. Melker Hagsäter, Thomas Glasdam Jensen, Henrik Bruus and Jörg P. Kutter, *Acoustic resonances in microfluidic chips: full-image micro-PIV experiments and numerical simulations*, Lab Chip 7, 1336–1344 (2007).
- [2] S. Melker Hagsäter, Andreas Lenshof, Peder Skafte-Pedersen, Jörg. P. Kutter, Thomas Laurell, and Henrik Bruus, *Acoustic resonances in straight micro channels: Beyond the 1D-approximation*, Lab Chip 8, 1178–1184 (2008).
- [3] Otto Manneberg, S. Melker Hagsäter, Jessica Svennebring, Hans M Hertz, Jörg P Kutter, Henrik Bruus, Martin Wiklund, *Spatial confinement of ultrasonic force fields in microfluidic channels*, Ultrasonics, dx.doi.org/10.1016/j.ultras.2008.06.012 (2008).
- [4] Henrik Bruus, *Theoretical Microfluidics*, Oxford University Press (Oxford, 2008).

Acoustic streaming: The main driving mechanism for particle clump formation in MHz ultrasonic standing waves

Jeremy J Hawkes¹ and Rito Mijarez Castro²

¹ School of Chemical Engineering and Analytical Science
The University of Manchester
PO Box 88, Sackville Street
Manchester M60 1 QD

²Gerencia de Control e Instrumentación, Instituto de
Investigaciones Eléctricas, CP 62490 Cuernavaca,
Morelos, México



“The cause of these effects” (clouds formed of fine particles in air between nodal lines) is “When a plate is made to vibrate, currents are established in the air lying upon the surface of the plate, which pass from the quiescent lines towards the centres or lines of vibration, that is, towards those parts of the plates where the excursions

are greatest, and then proceeding outwards from the plate to a greater or smaller distance, return towards the quiescent lines.”

Michael Faraday 1831 [1 p302]

When Faraday described particles forming clouds in air currents he was describing small particles moving on or just above plates in the opposite direction to larger heavier particles which move to the nodal positions to produce Chladni figures[2]. 35 years later Kundt[3] moved particles in an airborne standing wave, and Dvorak[4] observed a continuous streaming of the fluid in the tubes from the nodes to the antinodes in the centre of the tube and in the opposite direction along the walls (shown in figure 1a). He saw that clumps were formed by acoustic streams. In 1888 Rayleigh[5] recognised that these were driven by the same acoustic streams described by Faraday[1]. These streams with quarter wavelength dimensions occurring between nodes are now called Rayleigh streaming.

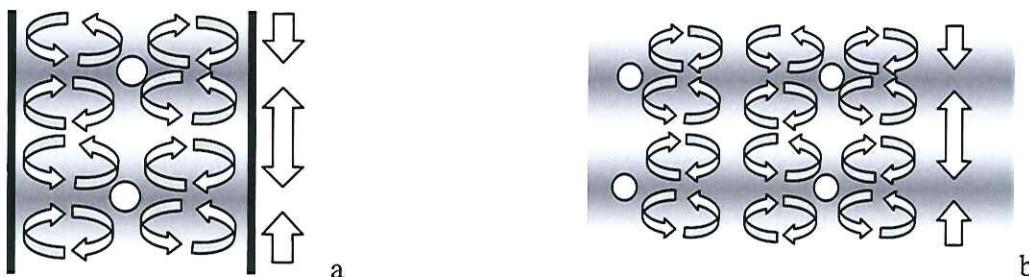


Figure 1 Streaming is represented by the curved arrows. The standing wave radiation force is marked by the straight arrows and shading shows the pressure nodes of this force. Clumping positions are marked by the circles. a) Streaming described by Dvorak in a Kundt tube. b) Streaming in a wide aspect channel, where the lateral wavelength is less than half the chamber width.

In the twentieth century many other clumping mechanisms were discovered and proposed. Most of these fall into two types

- 1 Clumps formed by particles driven along a gradient in the sound field [5, 6, 7, 8] either towards nodes in standing waves resonating at right angles to the main node producing the striations. Or simply by a gradient in the sound intensity. Either of these can easily occur the resonant case is of course helped by good reflections from rigid walls. Some systems have been designed to produce such waves at right angles either by the chambers shape or by using two transducers at right angles. However as figure 2 shows experimental results do not always fulfil expectations when streaming is not taken into account. In some systems small particles are observed moving in the opposite direction to large particles, this can be explained by an interaction between streaming and acoustic force but not acoustic forces alone.

- 2 Clumps formed by interaction between particles, four mechanisms are known: i) scattering of sound on the particles, particle wakes and orthokinetic forces (collision of unequal particles due to differential entrainment) [9,10, 11, 12] and Bjerknes forces operating on bubbles and oscillating particles [13, 14]. Most particle-particle forces operate in both standing and travelling waves, on particles in close proximity [15]; and are most effective at lower frequencies. They may alter the rate of clump formation but are unlikely to influence the final location of the clumps.

Returning to Dvorak and Rayleigh. The streaming units have $\frac{1}{4}$ wavelength dimensions. Between nodes the wavelength is clear, in the lateral direction Dvorak and Rayleigh used tubes with a half wavelength width. In the common short pathlength tubes used today the aspect ratio often supports many wavelengths in the lateral direction but the wavelength (determined by clump position) is not usually the same as the wavelength through the fluid in the vertical direction. Evidence will be given to show this wavelength is in the driving plate not the fluid.

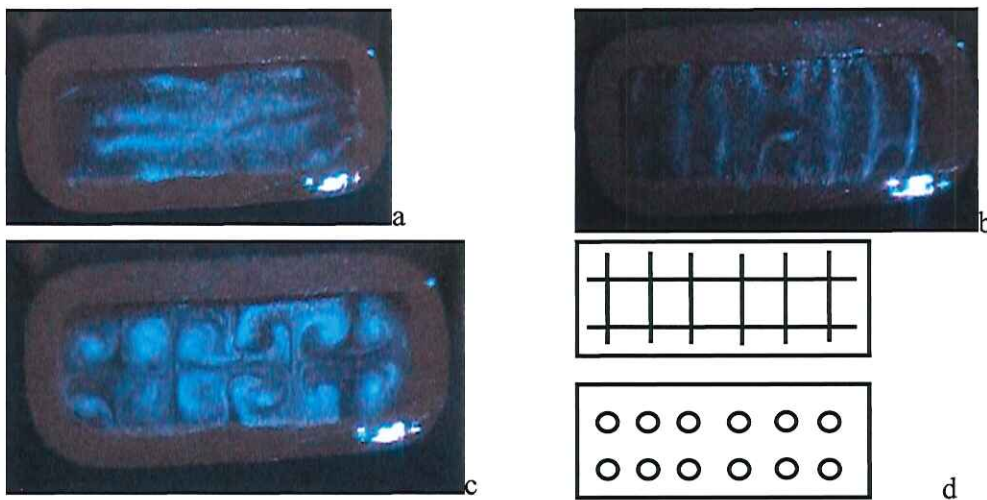


Figure 2 Aerosol emerging from a rectangular duct in which the air in the cavity is resonating in a) the width direction, b) the length direction c) the width and length directions. d) Crossing nodes and clumping positions expected in (c) in the absence of streaming.

It is complicated to have particle position determined by a combination of radiation forces and streaming. In the case of liquid droplets in air a further level of complexity arises because of streaming within the droplets and reversing the direction of force experienced by the droplets[16].



Figure 3 Two aerosol emerging from a tube vibrating to produce the same resonance in the cavity. a) water droplets $\sim 5 \mu\text{m}$ diameter, b) smoke particles $\sim 2 \mu\text{m}$ diameter.

References

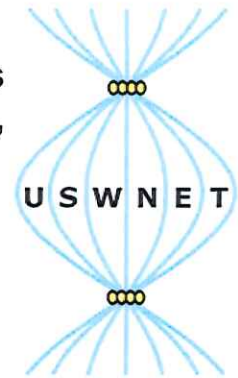
- 1 M. Faraday, On a Peculiar Class of Acoustical Figures; and on Certain Forms Assumed by Groups of Particles upon Vibrating Elastic Surfaces. *Philosophical Transactions of the Royal Society of London*, 121. (1831), 299-340.
- 2 E. Chladni. Entdeckungen ueber die Theorie des Klanges, Discoveries Concerning the Theory of Music 1787.
- 2 A. Kundt, Ann.d. Physik 128 (1866) 337
- 3 Dvorak Ann. D. Physik 1501873

- 4 Lord Rayleigh. On the Circulation of Air Observed in Kundt's Tubes, and on Some Allied Acoustical Problems
Philosophical Transactions of the Royal Society of London, 175 (1884) 1-21.
- 5 S.M. Woodside, J. Piret, M. Gröschl., E. Benes, B.D. Bowen, Acoustic force distribution in resonators for ultrasonic particle separation, *AIChE J.* 44 (1998) 1976-1984.
- 6 A. Hancock, M.F. Insana, and J.S. Allen, Microparticle column geometry in acoustic stationary fields, *J. Acoust. Soc. Am.* 113 (2003) 652-659.
- 7 T. Tuziuti, T. Kozuka and H. Mitome Measurement of distribution of Acoustic Radiation Force Perpendicular to Sound Beam, *Jpn. J. Appl. Phys* 38 (1999) 3297-3301.
- 8 G. Whitworth and W.T. Coakley, Particle column formation in a stationary ultrasonic field, *J Acoust Soc. Am.* 91 (1992) 79-85.
- 9 O. A. Ezekoye and Y. W. Wibowo Simulation of acoustic agglomeration using a sectional algorithm, *J. Aerosol Sci.* 30 (9) (1999) 1117-1138.
- 10 M.A.H. Weiser and R.E. Apfel, E.A. Neppiras, Interparticle forces on red-cells in a standing wave field, *Acustica* 56 (1984) 114.
- 11 T.L. Hoffmann and G.H. Koopmann, Visualization of acoustic particle interaction and agglomeration: Theory evaluation, *J Acoust. Soc. Am.* 101 (1997) 3421-3429.
- 12 W.L Nyborg, Theoretical criterion for acoustic aggregation, *Ultrasound in Medicine and Biology* 15 (1989) 93-99.
- 13 T.J. Matula, S.M. Cordry, R.A. Roy, and L.A. Crum The Bjerknes force and bubble levitation under single-bubble sonoluminescence conditions, *J. Acoust. Soc. Am.* 102 (1997) 1522-1527.
- 14 W.König, Hydrodynamisch-akustische Untersuchungen:II. Über die Kräfte zwischen zwei Kugeln in einer schwingenden Flüssigkeit und über die Entstehung der Kundt'schen Staubfiguren, *Ann. Phys. Chem* 42 (1891) 549-563.
- 15 Nyborg W.L, Physical Principles of ultrasound. In: Fry FJ (ed.) *Ultrasound: Its Applications in Medicine and Biology*, Part I, Elsevier, Amsterdam, 1978 1 pp. 1-75.
- 16 H. Zhao, S.S. Sadhal and E.H. Trinh, Internal circulation in a drop in an acoustic field *JASA* 106 (1999)

1-Dimensional Transducer model for performance studies of ultrasonic standing waves in arbitrary stacks of PZT, liquid and solid layers

Frederic Cegla

Department of Mechanical Engineering
Imperial College London
Exhibition Road
South Kensington
London SW7 2AZ
United Kingdom
f.cegla@imperial.ac.uk

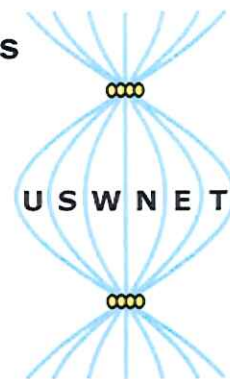


A 1-dimensional model of arbitrary stacks of material containing a piezo electric element is presented. The model predicts the electrical input impedance of the piezo element (PZT) taking into account the influence of the mechanical coupling to all of the adjacent layers. Calculations are based on a transfer matrix approach and allow the prediction of the amplitude of the vibration due to a unit voltage applied across the PZT terminal at any point in the stack over a chosen frequency range. This can also be visualised as a plot of the pressure, displacement or velocity distribution across the whole stack at a certain frequency. The model is useful for parametric analysis of different test cell designs of ultrasonic chambers, allowing the visualisation of the influence of changes in different physical or geometric properties of individual components within the stack. A detailed analysis of a specific ultrasonic chamber and its sensitivity to fluid temperature is presented. Results are summarised in plots of the resonant frequency and maximum pressure in the liquid layer against temperature.

Numerical simulations for the time-averaged acoustic forces acting on rigid circular cylinders in ideal and viscous fluids

Jingtao Wang, Jürg Dual

Institute of Mechanical Systems
Dept. of Mechanical and Process Eng.
ETH Zurich
CH-8092 Zurich
Switzerland
wang@imes.mavt.ethz.ch



Introduction

The time-averaged acoustic force can be applied to many practical fields such as acoustic sensors, ultrasonic levitation and contactless particle manipulation [1, 2] which has become a hot research topic in the field of ultrasonic devices. It is necessary to accurately predict the mean forces on suspended obstacles including the primary force and the secondary force to design ultrasonic particle manipulators. Although there have been many analytical solutions on this topic, it is difficult to determine the acoustic forces on obstacles under more complex system conditions such as proximity to the chamber wall, complex viscous function, acoustic streaming and complicated particle shapes. Therefore, the numerical modelling may become a powerful tool. In this paper, efforts are made to calculate the time-averaged forces on one or two rigid cylinders in ideal and viscous fluids exerted by a standing sound wave field by solving the N-S equations directly using FVM [3] (Finite Volume Method) techniques. The reason why we use FVM here rather than commercial software packages such as COMSOL is that we find FVM method takes much less computation time than them from our preliminary numerical tests. The results are compared with the theoretical prediction, COMSOL simulations and Haydock's [4] simulations. The viscous effects of the host medium are also investigated in detail.

Results in inviscid fluid

We first calculate the cases without viscosity with geometry configurations according to Fig. 1. To make comparison, we also calculate all the cases by a commercial FEM software package named COMSOL. Details of the results are given in Tab.1 for different particle radius.

The results of several methods for the cases without perfectly matched layers (PMLs) are listed in Tab. 1. It can be seen in Tab. 1 that the results between our FVM program and COMSOL agree with each other very well. The maximum relative difference is 3.1%. Meanwhile, the lattice Boltzmann (LB) method [4] gives quite different results compared with FVM and COMSOL. The density contours calculated by our FVM program at time $100T$ are plotted in Fig. 1.

Results in viscous fluid

In Tab. 2, we present the results from FVM with PMLs at the cylinder position $h = 375$ for radius from 5 to 80 with four different viscosities 0.0, 0.167, 0.835 and 1.67. The PMLs eliminate all reflections from the bottom ($y = 0$) and top ($y = y_{\max}$) boundaries. The force ratios between the mean forces in the fluid with different viscosities and in the inviscid fluid for different radii are plotted in Fig. 2. Obviously, from Fig. 2, the viscosity of the host medium influences the mean forces more significantly at the small cylinders for a certain wave frequency, which is also described by analytical works.

Figure 3 presents the velocity vectors of the acoustic streaming around the cylinder in the case $R = 20$. The streaming field is asymmetric about the cylinder in the horizontal direction, because the cylinder

locates at the midway between a velocity node and its next anti-node. There are four vortices away from the cylinder boundary as described by Nyborg [5].

Tab. 1 Acoustic radiation forces for the cases without PML. (F_{th} : theoretical solutions, F_{LB} : calculated by LB method F_{COM} : calculated by COMSOL, F_{FVM} : calculated by our FVM program)

R	L_y	L_x	h	$F_{th} (10^{-5})$	$F_{LB} (10^{-5})$	$F_{COM} (10^{-5})$	$F_{FVM} (10^{-5})$
5	100	1000	375	-1.24	-3.04	-1.22	-1.25
10	100	1000	375	-4.95	-8.20	-5.13	-5.17
20	200	1000	375	-19.79	-25.12	-21.13	-21.17
40	200	1000	375	-77.85	-81.02	-108.41	-105.15
80	500	1000	375	-265.70	-247.20	-384.22	-375.30

Tab.2 Mean forces for the viscosity versus the radius ($\times 10^{-5}$)

$R \backslash \nu$	5	10	20	40	80
0.0	-1.22	-5.09	-19.83	-80.33	-303.96
0.167	-3.01	-8.21	-26.04	-90.48	-316.15
0.835	-4.96	-11.60	-31.89	-102.45	-314.03
1.670	-6.33	-13.89	-33.08	-107.59	-319.17

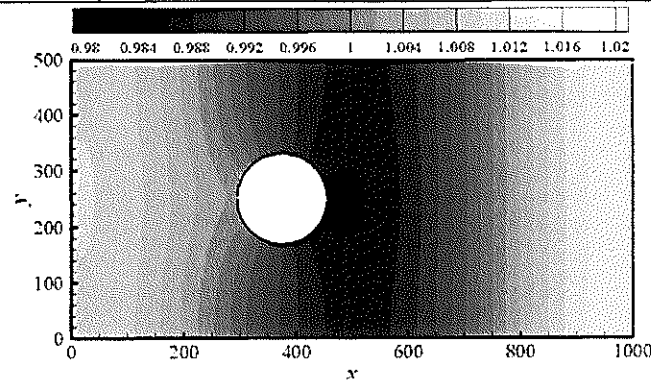


Fig. 1 The density distribution at time 100T.

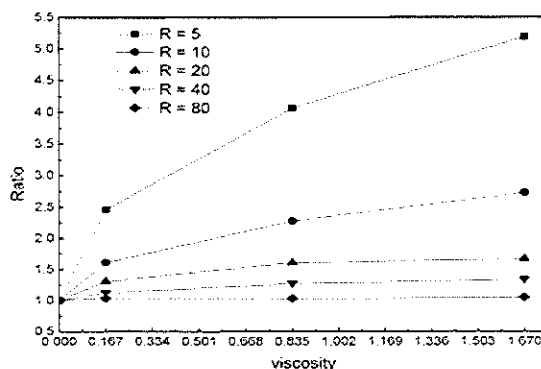


Fig. 2 Force ratios for different cases.

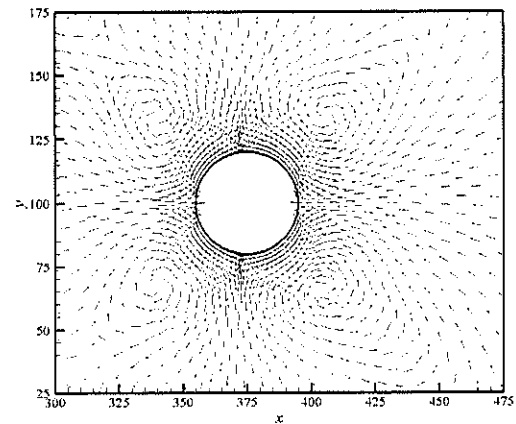
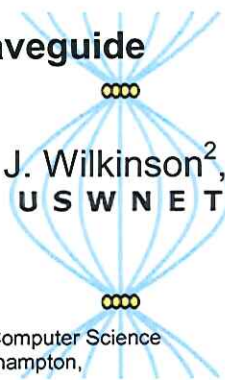


Fig. 3 Velocity vectors of the acoustic streaming around the cylinder ($R = 20$).

1. Haake, A., et al., *Positioning, displacement, and localization of cells using ultrasonic forces*. Biotechnology and bioengineering, 2005. **92**(1): p. 8-14.
2. Laurell, T., F. Petersson, and A. Nilsson, *Chip integrated strategies for acoustic separation and manipulation of cells and particles*. Chemical Society Reviews, 2007. **36**(3): p. 492-506.
3. Jameson, A. and D. Mavriplis, *Finite volume solution of the two-dimensional Euler equations on a regular triangular mesh*. AIAA paper 85-0435, 1985.
4. Haydock, D., *Lattice Boltzmann simulations of the time-averaged forces on a cylinder in a sound field*. Journal of Physics A: Mathematical and General, 2005. **38**: p. 3265-3277.
5. Nyborg, W.L.M., *Acoustic streaming*. Physical Acoustic, edited by W. Mason (Academic, New York, 1965), 1965. **Vol. IIB**: p. 265-331.

Multi-modal particle manipulation with integrated optical waveguide detection

P. Glynn-Jones¹, R. Townsend¹, M. Hill¹, F. Zhang², L. Dong², J. Wilkinson², T. Melvin², N. Harris³



¹School of Engineering Sciences,
University of Southampton,
SO17 1BJ,
UK

P.Glynn-Jones@soton.ac.uk

²Optoelectronics Research Centre,
University of Southampton,
SO17 1BJ,
UK

³Electronics and Computer Science
University of Southampton,
SO17 1BJ,
UK

We present recent developments from the University of Southampton. A multi-modal acoustic particle manipulation device has been developed, permitting particles to be pushed against and pulled away from an optical waveguide that has been integrated into the glass reflector of a layered standing wave device. An evanescent field is produced by the laser pumped waveguide, leading to applications in fluorescent bio-assays – particularly those based on microbeads. By switching rapidly between modes it has been shown possible to manipulate particles to arbitrary positions within the chamber. We also show how particles can be distinguished based on the time they take to arrive at the waveguide after first being moved to the centre of the chamber – useful in multiplexing and sensing applications.

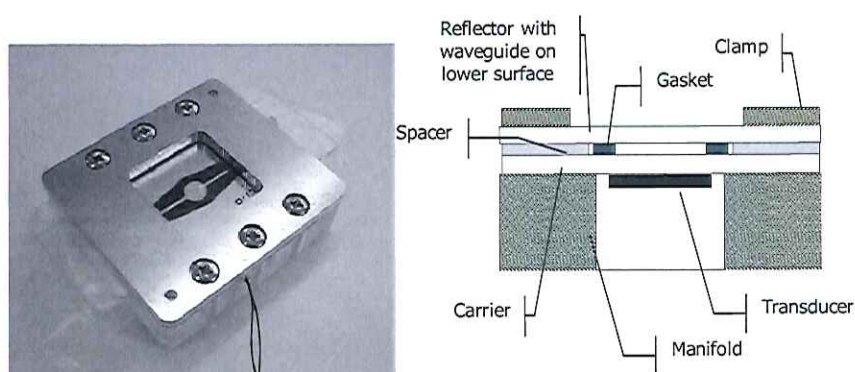


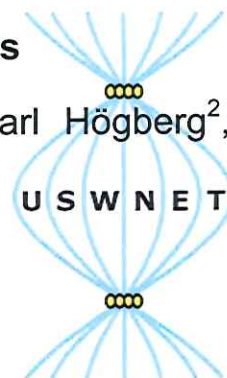
Fig. 1 Multi-modal particle manipulation device with integrated optical waveguide

A bioassay for monitoring ATP release in RBC agglomerates

Björn Hammarström¹, Chi-Manh Tran¹, Mikael Evander¹, Carl Högberg², David Erlinge², Thomas Laurell¹, Johan Nilsson¹

¹Department of Electrical Measurements
Lund University
P.O. Box 118, 221 00 Lund
Sweden
bjorn.hammarstrom@elmat.lth.se

²Department of Cardiology
Lund University
Lund
Sweden



Standing ultrasonic waves can be utilized to form cell agglomerates. Noncontact handling of a finite number of cells in combination with a microfluidic perfusion system offers a precisely controlled cell microenvironment¹. This provides new possibilities to advance biological understanding by enabling new kinds of bioassays.

Red blood cells (RBC) were ultrasonically trapped in a 75 μm high glass reflector channel with a resonator frequency of 10 MHz and studied with the aim of identifying ATP release mechanisms. The ATP concentration in blood mediates the vascular diameter by triggering release of nitric oxide in the endothelium². Increased concentrations of nitric oxide will relax smooth muscle cells surrounding the blood vessel and allow the vascular diameter to expand. Since RBCs constitute 45 % of the total blood volume their mechanisms of ATP release is suspected to be highly relevant in this context.

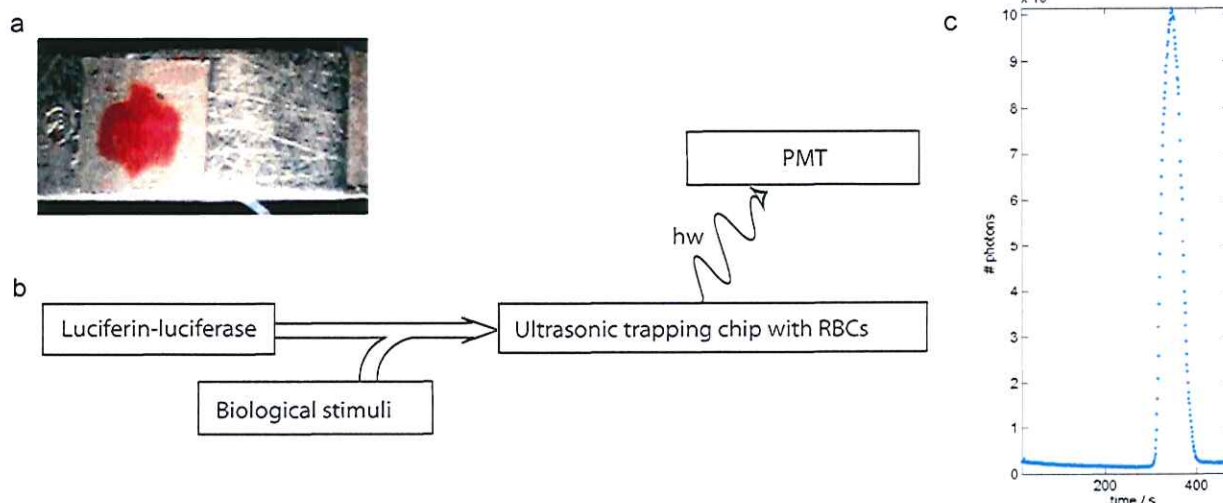


Fig. 1; (a) an acoustically trapped RBC agglomerate, (b) the detection scheme used to monitor the RBC ATP response and (c) measurement curve of ATP release during lysis of RBC.

The RBC agglomerate was perfused with a luciferin-luciferase solution. The luminescent reaction between ATP and luciferin was used to monitor ATP released by the agglomerate. By injecting biological stimuli into the luciferin-luciferase solution the dynamics of RBC ATP response was recorded. The system was used to test ATP responses to lysis, ethanol and adrenaline and in these cases increased levels of ATP has been recorded.

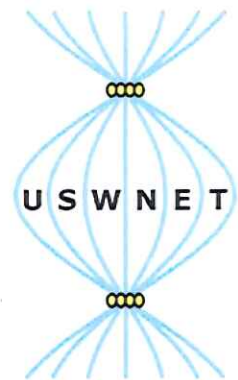
¹ M. Evander, L. Johansson, T. Lilliehorn, J. Piskur, M. Lindvall, S. Johansson, M. Almqvist, T. Laurell and J. Nilsson, "Noninvasive acoustic cell trapping in a microfluidic perfusion system for online bioassays", *Analytical Chemistry* 79, 2984-2991 (2007)

² Alexander K. Price, R. Scott Martin, Dana M. Spence, "Monitoring erythrocytes in a microchip channel that narrows uniformly: Towards an improved microfluidic-based mimic of the microcirculation", *Journal of Chromatography A* 1111, 220-227 (2006)

Chip-integrated Confocal Ultrasonic Resonator for Selective Bioparticle Manipulation

Jessica Svennebring, Hans M. Hertz and Martin Wiklund

Royal Inst. of Technology (KTH)
Dept. of Applied Physics.
KTH/AlbaNova
SE-10691 Stockholm
Sweden
jessica.svennebring@biox.kth.se



Confocal or hemispherical ultrasonic resonators are focused standing-wave manipulation systems based on curved reflector elements. Such resonator designs have previously been employed in macro-scale systems for trapping of mm-size objects in air¹, and of μm -size objects in fluid suspensions.² The curved reflector elements create a focused resonant acoustic field with strong radiation forces in all directions, which makes it possible to trap objects three-dimensionally.³ On the other hand, emerging chip-based ultrasonic manipulation systems typically employ plane-parallel resonators (e.g., microchannels with constant cross-sections.) In the present paper, we demonstrate a confocal ultrasonic resonator integrated in a microfluidic chip for selective manipulation of cells or other bioparticles.

The confocal resonator consists of a microfluidic expansion chamber where the channel walls are two cylindrical segments separated by twice their radius of curvature $2R = 4.92\text{ mm}$ (cf. Fig. 1). The expansion chamber is reached by straight inlet and outlet channels with widths 0.33 mm . The ultrasound is coupled into the chip by two external wedge transducers⁴ operating at 4.6 and 6.9 MHz (cf. Fig. 1). The 4.6-MHz and 6.9-MHz resonances are used for particle pre-alignment into two or three nodes in the straight inlet channel, respectively. In addition, the 6.9-MHz resonance is also used for particle trapping and positioning in the center of the expansion chamber. Since the chip is compatible with any kind of high-resolution optical microscopy, it can be used for detailed optical characterization of trapped cells.

In Fig. 2 we demonstrate a set of manipulation functions used for selection and positioning of cells or other bioparticles. The process begins with pre-alignment into two nodes at 4.6-MHz , 10-V_{pp} actuation, resulting in bypassing of particles through peripheral streamlines in the expansion chamber (Fig. 2a). Then, by switching to 6.9-MHz , 10-V_{pp} actuation, particles are pre-aligned into three nodes (Fig. 2b). The central of the three nodes is used for injection of particles into the streamline crossing the center of the expansion chamber. Finally, by actuation of both transducers simultaneously (at 4.6 and 6.9 MHz , same voltage levels as previous), the injected particles are trapped, aggregated and retained close to the center of the expansion chamber (Fig. 2c). In the pre-alignment channel, the 4.6-MHz resonance is dominating over the 6.9-MHz resonance at the applied voltages, which results in two-node alignment and bypassing of all new incoming particles in the chamber (Fig. 2c). Since the 6.9-MHz actuation also matches with a half-wave resonance in the vertical direction in the microchannel (of height 0.11 mm), the positioned particles are aggregated in horizontally oriented monolayers (Fig. 2d).

In Fig. 3, we demonstrate two examples of label-free imaging of an ultrasonically retained aggregate containing ~ 100 COS-7 cells: Phase contrast and dark-field microscopy. In addition, it is also possible to use epi-fluorescence characterization (cf. Fig. 2d, lower panel). Thus, the device is compatible with both functionality studies based on, e.g., fluorescent probes, as well as with label-free studies of, e.g., the morphology or topology of cells.

Since ultrasonic manipulation of cells in microfluidic chips has been shown to be a gentle and fully biocompatible method^{5,6}, we aim for using the device for dynamic (long-term) optical characterization of cells. For example, a sub-population of few up to hundreds of cells may quickly be selected, aggregated and positioned in the expansion chamber from a continuous feeding flow of a cell suspension, followed by bypassing of excess cell sample.

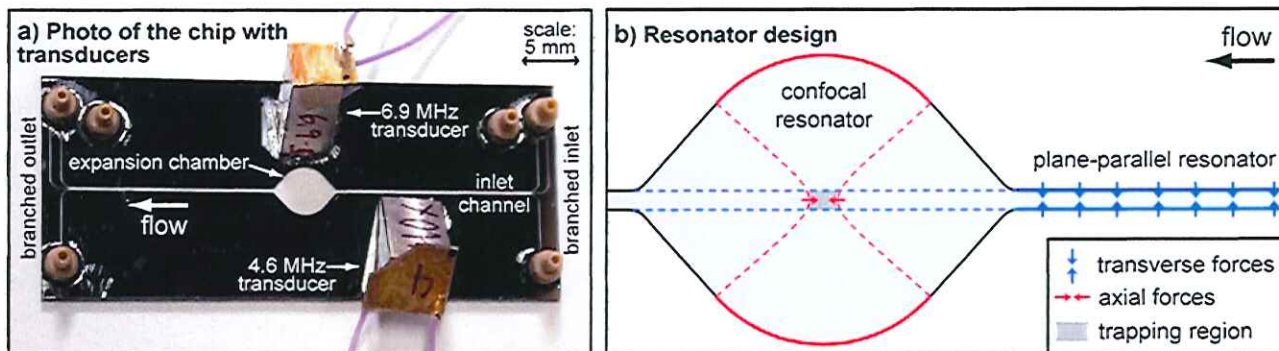


Fig. 1: Photograph and illustration of the resonator design.

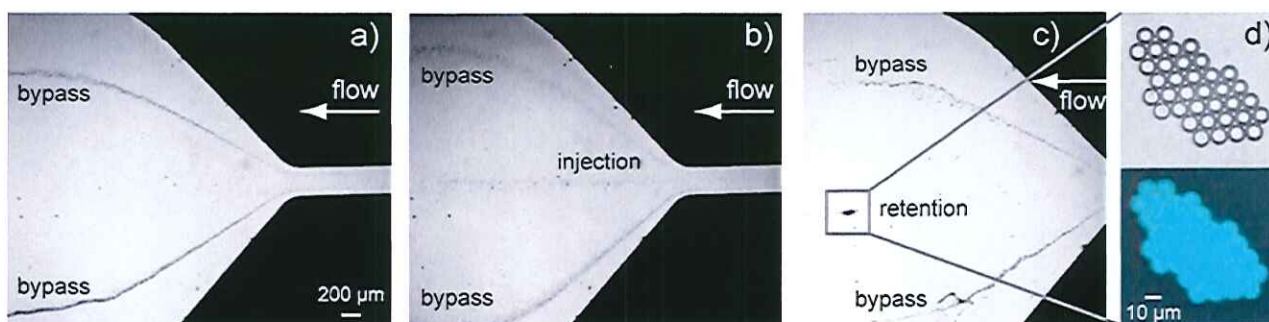


Fig. 2: Demonstration of selective particle manipulation during fluid flow: (a): Bypassing of 10- μm polystyrene particles at 4.6-MHz actuation. (b): Injection of particles to the center of the expansion chamber at 6.9-MHz actuation. (c): Retention and positioning of particles while bypassing excess particles at combined 4.6-MHz and 6.9-MHz actuation. (d): Positioning of a monolayer aggregate, imaged by transmission light (upper panel) and fluorescence (lower panel) microscopy. The scalebar in (a) applies to Figs 2a through (c).

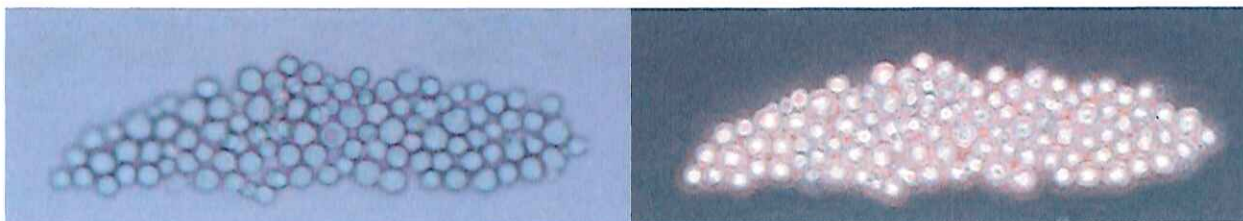


Fig. 3: Imaging of a trapped and retained monolayer aggregate of COS-7 cells, imaged by phase contrast (left), and dark field (right) microscopy. The size of the cell aggregate is $220 \times 60 \mu\text{m}^2$

- ¹ E. H. Brandt, "Levitation in Physics", *Science* **243**, 349-355 (1989).
- ² M. Wiklund et al, "Ultrasonic enrichment of microspheres for ultrasensitive biomedical analysis in confocal laser-scanning fluorescence detection", *J. Appl. Phys.* **96**, 1242-1248 (2004).
- ³ H. M. Hertz, "Standing-wave acoustic trap for noninvasive positioning of microparticles", *J. Appl. Phys.* **78**, 4845-4849 (1995).
- ⁴ O. Manneberg et al, "Wedge transducer design for two-dimensional ultrasonic manipulation in a microfluidic chip", accepted for publication in *J. Micromech. Microeng.* (2008).
- ⁵ J. Hultström et al, "Proliferation and viability of adherent cells manipulated by standing-wave ultrasound in a microfluidic chip", *Ultrasound Med. Biol.* **33**, 145-151 (2007).
- ⁶ J. Svennebring et al, "Temperature regulation during ultrasonic manipulation for long-term cell handling in a microfluidic chip", *J. Micromech. Microeng.* **17**, 2469-2474 (2007).

X-ray structural analysis in the therapy and diagnosis of urolithiasis

Kamelia STANOEVA, Ivan GEORGIEV, Maria IVANOVA

Medical University – Sofia
Dept. of Chemistry and Biochemistry
Sofia, Bulgaria
kamelia.stanoeva@gmail.com

Introduction:

Renal stones (urolithiasis) is a socially significant disease, especially common in developed countries, attaining people in active age: 30-50years old. Therefore the analysis of its ethiology and pathological mechanisms is very important. Different analytical methods including physical, chemical, mechanical, physico-chemical assays are widely used in urology.

Aim:

The aim of our study was to identify the efficacy and the adequacy of results obtained by X-ray analysis¹ used as an analytical method in urolithiasis. Data from kidney stones gathered from the 1989 onwards in the Medical University – Sofia hospitals was checked and methods used were compared.

Methods:

Data from renal stones analysed by X-ray is compared to other standard methods in urolithiasis. Accuracy, time needed for a result, accessibility of the technique were evaluated. According to the popular chemical classification of renal stones (urates, oxalates, phosphates, cystines) our aim was to cover data from all known types of pure and mixed calculi originating from different patients, male and females, in different age groups.

Crystalline interplanar spacings, already known and irreproducible for another crystals are used in the basis of the physical X-ray analysis. Debaegramms obtained are standartly read in a specialised laboratory of the Bulgarian Academy of Sciences. Data is then digitally compared to other assays of the same samples and information in clinical record.



Fig.1 Renal calculi samples

Results:

Clinical exams performed in situ after operations reveal over 30% of wrong diagnoses in hospitals using direct chemical analytical methods (data extracted from medical records and samples checked by other methods).

X-ray analysis can be performed on calculi as small as 2mg² which makes it a precise method and in certain cases the only diagnostical method to be used in situ. This technique demands relatively short time for stone determination compared to chemical assays of 24 hours. The results show not the only the basic type of lithiasis as common tests but also secondary crystals inside. The study shows that practically all examined stones are of mixed type with prevalence of certain crystals – information unattainable by other chemical methods.

Conclusions:

Bearing in mind the high prevalence of urolithiasis on the Balkans and in Europe as a whole, the early diagnosis is of vital importance. Novel therapies allow to interfere with the formation of the calculi inside the kidneys. In order to use these advanced pharmaceutical products, the type of kidney stones should be accessed on an early stage and without operation, which can be easily achieved using X-ray analysis.

USWNet 2008 - 13th-14th November 2008 - ETH Zurich - Switzerland

Participants		Role	Affiliation	Email
1 Augustsson	Per		Lund University	per.augustsson@elmat.lth.se
2 Bjelobrk	Nana		ETH Zurich	nadab@ethz.ch
3 Boltryk	Rosemary	ORG	University of Southampton	R.J.Boltryk@soton.ac.uk
4 Bruus	Henrik		Technical Univeristy of Denmark	henrik.bruus@nanotech.dtu.dk
5 Burg	Brian		ETH Zurich	bburg@ethz.ch
6 Cegla	Frederic		Imperial College London	f.cegla@imperial.ac.uk
7 Dual	Jürg	ORG	ETH Zurich	juerg.dual@imes.mavt.ethz.ch
8 Garbin	Valeria		University of Twente	v.garbin@utwente.nl
9 Gedge	Michael		University of Southampton	mjg305@soton.ac.uk
10 Glynn-Jones	Peter		University of Southampton	P.Glynn-Jones@soton.ac.uk
11 Goksör	Matthias	INV	Göteborg University	mattias.goksor@physics.gu.se
12 Gomez	Tomas E.		Spanish Scientific Research Council	tgomez@ia.cetef.csic.es
13 Gonzalez Gomez	Iciar		Spanish Scientific Research Council	iacgg38@ia.cetef.csic.es
14 Grenvall	Carl		Lund University	carl.grenvall@elmat.lth.se
15 Gutmann	Oliver		Roche Diagnostics Ltd.	oliver.gutmann@roche.com
16 Hammarström	Björn		Lund University	bjorn.hammarstrom@elmat.lth.se
17 Harris	Nick		University of Southampton	nrh@ecs.soton.ac.uk
18 Hawkes	Jeremy	ORG	The University of Manchester	J.Hawkes@manchester.ac.uk
19 Hay	Todd		University of Twente	haymeister@gmail.com
20 Hertz	Hans		KTH Stockholm	hans.hertz@biox.kth.se
21 Hill	Martyn	ORG	University of Southampton	M.Hill@soton.ac.uk
22 Holsteyns	Frank Ludwig		Sez Ltd.	f.holsteyns@at.sez.com
23 Jaeger	Magnus	INV	Fraunhofer Inst. For Biomedical Engineering	magnus.jaeger@ibmt.fraunhofer.de
24 Jayasekera	Pramukh		DSTL Porton Down	pjayasekera@dstl.gov.uk
25 Johannsson	Linda		Uppsala University	linda.johansson@angstrom.uu.se
26 Koch	Cosima		TU Wien	cosima.koch@tuwien.ac.at
27 Laurell	Thomas		Lund University	thomas.laurell@elmat.lth.se
28 MacDonald	Michael P		University of Dundee	m.p.macdonald@dundee.ac.uk
29 Manneberg	Otto		KTH Stockholm	otto.manneberg@biox.kth.se
30 McDonnell	Martin		DSTL Porton Down	mbmcdonnell@dstl.gov.uk
31 Möller	Dirk		ETH Zurich	dirk.moeller@imes.mavt.ethz.ch
32 Narayanan	Chidambaram		ASCOMP GmbH	chidu@ascomp.ch
33 Nilson	Johan		Lund University	johan.nilsson@elmat.lth.se
34 Oberti	Stefano	ORG	ETH Zurich	stefano.oberti@imes.mavt.ethz.ch
35 Radel	Stefan		TU Wien	stefan.radel@tuwien.ac.at
36 Schwarz	Thomas		ETH Zurich	schwarz@imes.mavt.ethz.ch
37 Stanoeva	Kamelia		Medical University-Sofia	kamelia.stanoeva@gmail.com
38 Svennebring	Jessica		KTH Stockholm	jessica.svennebring@biox.kth.se
39 Trippa	Giuliana		University of Oxford	giuliana.trippa@eng.ox.ac.uk
40 Versluis	Michel		University of Twente	m.versluis@utwente.nl
41 Wang	Jingtao		ETH Zurich	wang@imes.mavt.ethz.ch
42 Wiklund	Martin	ORG	KTH Stockholm	martin.wiklund@biox.kth.se
43 Zourob	Mohammed		Biophage Pharma	m.zourob@biophagepharma.net

ORG organisation committee member

INV invited speaker